# Interaction of a Bacterially Expressed Peptide from the Receptor Binding Domain of *Pseudomonas aeruginosa* Pili Strain PAK with a Cross-Reactive Antibody: Conformation of the Bound Peptide†

A. Patricia Campbell,*,‡ Wah Y. Wong,§,|| Randall T. Irvin,§,|| and Brian D. Sykes§,⊥

*Department of Medicinal Chemistry, School of Pharmacy, University of Washington, Seattle, Washington 98195, Protein Engineering Network of Centers of Excellence, University of Alberta, Edmonton, Alberta T6G 2S2, Canada, Department of Medical Microbiology and Immunology, University of Alberta, Edmonton, Alberta T6G 2H7, Canada, and Department of Biochemistry, University of Alberta, Edmonton, Alberta T6G 2H7, Canada*

*Received July 17, 2000; Revised Manuscript Received September 19, 2000*

ABSTRACT: The C-terminal receptor binding region of *Pseudomonas aeruginosa* pilin protein strain PAK (residues 128−144) has been the target for the design of a vaccine effective against *P. aeruginosa* infections. We have recently cloned and expressed a $^{15}$N-labeled PAK pilin peptide spanning residues 128−144 of the PAK pilin protein. The peptide exists as a major (trans) and minor (cis) species in solution, arising from isomerization around a central Ile$^{138}$-Pro$^{139}$ peptide bond. The trans isomer adopts two well-defined turns in solution, a type I $\beta$-turn spanning Asp$^{134}$-Glu-Gln-Phe$^{137}$ and a type II $\beta$-turn spanning Pro$^{139}$-Lys-Gly-Cys$^{142}$. The cis isomer adopts only one well-defined type II $\beta$-turn spanning Pro$^{139}$-Lys-Gly-Cys$^{142}$ but displays evidence of a less ordered turn spanning Asp$^{132}$-Gln-Asp-Glu$^{135}$. These turns have been implicated in cross-reactive antibody recognition. $^{15}$N-edited NMR spectroscopy was used to study the binding of the $^{15}$N-labeled PAK pilin peptide to an Fab fragment of a cross-reactive monoclonal antibody, PAK-13, raised against the intact PAK pilus. The results of these studies are as follows: the trans and cis isomers bind with similar affinity to the Fab, despite their different topologies; both isomers maintain the conformational integrity of their $\beta$-turns when bound; binding leads to the preferential stabilization of the first turn over the second turn in each isomer; and binding leads to the perturbation of resonances within regions of the trans and cis backbone that undergo microsecond to millisecond motions. These slow motions may play a role in induced fit binding of the first turn to Fab PAK-13, which would allow the same antibody combining site to accommodate either trans or cis topology. More importantly for vaccine design, these motions may also play a role in the development of a broad-spectrum vaccine capable of generating an antibody therapeutic effective against the multiple strains of *P. aeruginosa*.

*Pseudomonas aeruginosa* is a Gram-negative rod-shaped bacterium that causes opportunistic respiratory tract infections in cancer, cystic fibrosis, and intensive care patients (*1*−*5*). The initial step in the pathogenicity of *P. aeruginosa* is adherence to the host cell via polar pili on the bacterial surface (*2*, *5*, *6*). The pili are proteinaceous filaments composed of a homologous polymer of pilin protein (*5*), where the semi-conserved C-terminal region of the last pilin monomer in the polymer array contains the actual binding domain for adherence to the host epithelium (*6*−*13*). The seven different strains of *P. aeruginosa* so far characterized share a common glycosphingolipid cell surface receptor (*7*, *14*−*17*) where the minimal structural element is a disaccharide $\beta$GalNAc(1−4) $\beta$Gal (*18*) to which the C-terminal region of the pilin monomer binds.

In counteracting *P. aeruginosa* infections, an anti-adhesin vaccine has been proposed. Antibodies specific for the pilin C-terminal region can be raised with synthetic peptides and can be used to counteract infection by blocking bacterial attachment (*19*). Since *P. aeruginosa* exists as seven different strains, production of a cross-reactive antibody effective against all strains would be most desirable for an antibody therapeutic. It is possible to envisage such a cross-reactive antibody since all strains bind to the same receptor and display a conserved antigenic epitope (*10*) within the receptor-binding region (adhesintope) of the pilus (*20*). In fact, anti-adhesin antibodies that recognize the adhesintope inhibit pilus/fimbrial-mediated adherence of *P. aeruginosa* and *Candida albicans* to asialo-GM-1 receptors and to human buccal epithelial cell surface receptors (*20*). In addition, the use of synthetic peptides has confirmed that the *P. aeruginosa* pilus adhesin and the *C. albicans* fimbrial adhesin possess a homologous receptor-binding domain (*21*).

† This work was funded by the Protein Engineering Network of Centres of Excellence (PENCE) and the Canadian Bacterial Diseases Network (CBDN), which are both funded by the Government of Canada.

* To whom correspondence should be addressed. Telephone: (206)-685-2468. Fax: (206)685-3252. E-mail: apc@u.washington.edu.

‡ Department of Medicinal Chemistry, University of Washington.

§ Protein Engineering Network of Centers of Excellence, University of Alberta.

|| Department of Medical Microbiology and Immunology, University of Alberta.

⊥ Department of Biochemistry, University of Alberta.

10.1021/bi0016568 CCC: $19.00 
Published on Web 11/10/2000

In an effort to understand the structural basis for this cross-reactivity of the pilin monomer with antibody and receptor, the NMR-free solution structures of four synthetic peptide antigens spanning the C-terminal receptor binding regions of four strains of *P. aeruginosa* pilin (PAK, PAO, KB7, and P1) were studied, and a common structural motif of two sequential $\beta$-turns was found (*22*, *23*). $^1$H NMR-monitored titrations of these four synthetic peptide antigens with a cross-reactive monoclonal antibody, Mab PAK-13, raised against the intact PAK pilus mapped the antigenic determinant to the two turns in all four peptides (*24*). The two turns were thus predicted to constitute the common structural element for cross-reactive antibody recognition. Transferred NOESY[1] experiments of these same four peptide antigens in complex with Mab PAK-13 were also performed to probe for conformational changes in the $\beta$-turns induced by binding to antibody (*24*). The bound peptide conformations were found to differ little from their free solution conformations, suggesting that the free peptide conformation is similar to the bound conformation and arguing for the role of a "flexible" combining site in cross-reactive antibody recognition.

Although these $^1$H NMR studies have provided interesting preliminary evidence of the involvement of the $\beta$-turns in cross-reactive antibody recognition of pilin antigens, they have been hampered by the inherent limitations of homonuclear two-dimensional NMR spectroscopy. The inclusion of $^{15}$N and $^{13}$C labels in the backbone and side chains of select pilin peptides would enable more sophisticated heteronuclear NMR experiments to be used in the study of this system. Isotope-edited NOESY and TRNOESY experiments of $^{15}$N/$^{13}$C-labeled pilin peptides bound to antibody would allow mapping of epitope regions of these peptides in order to determine if they involve both $\beta$-turns or indeed other binding motifs. $^{15}$N and $^{13}$C NMR relaxation experiments of the $^{15}$N/$^{13}$C-labeled pilin peptides in solution versus when bound to antibody would allow dynamical and motional information to be obtained for the peptides in their free versus bound conformations.

Toward these goals, a bacterial expression and purification system for recombinant pilin peptides was developed by Tripet et al. (*25*). This system was adapted to produce a $^{15}$N-labeled PAK pilin peptide spanning the C-terminal receptor-binding residues 128−144 of the intact PAK pilin monomer (Lys$^{128}$-Cys-Thr-Ser-Asp-Gln-Asp-Glu-Gln-Phe-Ile-Pro-Lys-Gly-Cys-Ser-Lys$^{144}$), and $^{15}$N-edited multidimensional NMR spectroscopy was used to determine the solution secondary structure of this peptide (*26*). The oxidized form of the recombinant PAK pilin peptide (containing the intramolecular disulfide bridge Cys$^{129}$- - -Cys$^{142}$) exists as a major (trans) and minor (cis) species in solution, arising from isomerization around a central Ile$^{138}$-Pro$^{139}$ peptide bond. The pattern of NOEs, temperature coefficients, and coupling constants observed for the trans isomer confirmed the presence of a type I $\beta$-turn and a type II $\beta$-turn spanning Asp$^{134}$-Glu-Gln-Phe$^{137}$ and Pro$^{139}$-Lys-Gly-Cys$^{142}$, respectively, in agreement with the NMR-free solution structure of the trans isomer of the synthetic PAK pilin peptide (*22*). In addition, the pattern of NOEs, temperature coefficients, and coupling constants observed for the cis isomer demonstrated a type II $\beta$-turn spanning Pro$^{139}$-Lys-Gly-Cys$^{142}$ and suggested a second $\beta$-turn spanning Asp$^{132}$-Gln-Asp-Glu$^{135}$. Apparently, the cis arrangement causes steric clashes between turns separated by only one residue and favors the formation of a first turn, which is displaced by two residues toward the N-terminus.

We report here the results of $^{15}$N-edited NMR studies of the $^{15}$N-labeled PAK pilin peptide in complex with the Fab fragment of PAK-13. These studies use a combination of chemical shift perturbation mapping, TRNOESY experiments, and measurement of coupling constants and temperature coefficients to probe for changes in the backbone conformations of the trans and cis isomers of the PAK pilin peptide occurring as a result of antibody binding. In a forthcoming paper (*27*), we will also report the results of $^{15}$N NMR relaxation studies of the $^{15}$N-labeled PAK pilin peptide in complex with Fab PAK-13. Taken together, these complimentary studies should provide a more detailed picture of the role of defined $\beta$-turn structure in antibody recognition and binding, while also exploring the role of peptide backbone motions on antibody cross-reactivity. A detailed structural and dynamical picture of PAK pilin immunogenicity will ultimately provide useful in the design of a potent synthetic peptide vaccine, immunospecific against *P. aeruginosa* infections, yet effective across the multiple strains of pilin.

## EXPERIMENTAL PROCEDURES

*Expression, Isotope-Labeling, and Purification of Recombinant PAK Pilin Peptide.* Details of the vector construction, cloning, expression, and purification of the $^{15}$N-labeled PAK pilin peptide have been previously described in detail (*25*, *26*). The sequence of the final $^{15}$N-labeled recombinant peptide construct was Lys$^{128}$-Cys$^{129}$-Thr$^{130}$-Ser$^{131}$-Asp$^{132}$-Gln$^{133}$-Asp$^{134}$-Glu$^{135}$-Gln$^{136}$-Phe$^{137}$-Ile$^{138}$-Pro$^{139}$-Lys$^{140}$-Gly$^{141}$-Cys$^{142}$-Ser$^{143}$-Lys$^{144}$-Hs$^{145}$, where Hs$^{145}$ indicates an additional homoserine residue at the C-terminus, a stable product of the cyanogen bromide cleavage of a methionine residue engineered into the end of the peptide sequence. Once isolated and purified, the recombinant peptide was oxidized to form an intramolecular disulfide bridge between residues Cys$^{129}$ and Cys$^{142}$, according to the protocol outlined in Campbell et al. (*22*).

*Production of Monoclonal Antibody, Mab PAK-13, and Its Fab Fragment.* Monoclonal antibody, Mab PAK-13, was prepared in mouse ascites as described previously (*10*, *28*). The Fab fragment of PAK-13 was then produced via papain digestion of purified IgG, using a procedure outlined in Campbell et al. (*24*).

*Competitive ELISA Assays of Recombinant PAK Pilin Peptide Binding to Mab PAK-13.* Competitive ELISA was carried out according to the protocol described by Wong et al. (*29*) in order to measure the apparent association constant ($K_a$) for the binding of the recombinant PAK pilin peptide to Mab PAK-13. The binding of the synthetic PAK pilin peptide to Mab PAK-13 was also measured for comparative purposes. Briefly described here, microtiter wells were coated with intact PAK pili and incubated at pH 7.2 with a solution

[1] Abbreviations: DSS, 2,2-dimethyl-2-sila-5-pentanesulfonate; ELISA, enzyme-linked immunosorbent assay; HSQC, heteronuclear single quantum coherence; NOE, nuclear Overhauser effect; NOESY, 2D nuclear Overhauser effect spectroscopy; TRNOE, transferred nuclear Overhauser effect; TRNOESY, 2D transferred nuclear Overhauser effect spectroscopy.

mixture of Mab PAK-13 and recombinant peptide (or synthetic peptide) at various concentrations of peptide. The $K_a$ for the association of peptide to PAK-13 was then calculated by the formula $K_a = 1/I_{50}$ as described by Nieto et al. (*30*).

*Preparation of NMR Samples and Issues of pH and Temperature.* Two separate peptide NMR samples were identically prepared by dissolving recombinant $^{15}$N-labeled PAK pilin peptide in 500 $\mu$L of 90% $H_2O$/10% $D_2O$ PBS buffer to a concentration of 1 mM, with DSS added as an internal chemical shift reference. Using NaOH and HCl solutions, the pH of the first sample was then adjusted to pH 7.2, and the pH of the second sample was adjusted to pH 4.5. The preparation of these separate peptide samples allowed all subsequent NMR experiments to be performed at both pH 7.2 and pH 4.5, enabling a determination of the effects of pH on peptide conformation and antibody recognition. In addition, as earlier NMR studies of the PAK pilin system had been performed at both pH 7.2 and pH 4.5,[2] a full synthesis of these earlier results with the present study required that both pH values be systematically investigated. Table 1 gives the $^1$H and $^{15}$N NMR resonance assignments for the trans and cis isomers of the recombinant $^{15}$N-labeled PAK pilin peptide at pH 4.5 and pH 7.2 and at a temperature of 5 °C.

The Fab PAK-13 to be used in the titration of the two $^{15}$N-labeled PAK pilin peptide samples was prepared in the following manner. The Fab PAK-13 solution described above was dialyzed against PBS buffer, pH 7.2, diluted 4:1 vol/vol in $H_2O$ to remove excess salts, and the dialysate lyophilized down to dryness. The powder was then dissolved in 50 $\mu$L of $H_2O$ to an approximate concentration of 3.5 mM, determined from an extinction coefficient at 280 nm of $\epsilon_{280} = 7.5 \times 10^7$ cm$^2$/mol (this corresponds to an estimated $OD_{280}$ of 1.5 at a concentration of 1 mg/mL). Two separate $^{15}$N-HSQC titrations were then performed, one using the first $^{15}$N-labeled PAK pilin peptide sample prepared at pH 4.5, and one using the second peptide sample prepared at pH 7.2. Aliquots of 10−20 $\mu$L were added to each peptide NMR sample, corresponding to 0.15 and 0.3 mol equiv of Fab/peptide. The pH was checked and readjusted to either pH 4.5 ± 0.02 or pH 7.20 ± 0.02 after each addition.

At the beginning and end of each titration (0.0 and 0.3 mol equiv of Fab/peptide), 3D $^{15}$N-edited HSQC NOESY and TRNOESY experiments were performed corresponding to four separate data sets (±Fab, pH 7.2 and pH 4.5) for each specified mixing time: (i) $^{15}$N-HSQC NOESY, pH 7.2, 5 °C, Fab/peptide = 0.0; (ii) $^{15}$N-HSQC TRNOESY, pH 7.2, 5 °C, Fab/peptide = 0.3; (iii) $^{15}$N-HSQC NOESY, pH 4.5, 5 °C, Fab/peptide = 0.0; and (iv) $^{15}$N-HSQC TRNOESY, pH 4.5, 5 °C, Fab/peptide = 0.3. Unfortunately, the signal-to-noise for the 3D NOESY spectra acquired at pH 7.2 was too poor to allow quantitative analysis, presumably due to an increased rate of amide proton exchange with bulk water at the higher pH. Thus, only the data from the NOESY and TRNOESY data acquired at pH 4.5 are presented in detail. Likewise, the 3D HNHA experiments performed at the beginning and end of each titration provided quantifiable data only at pH 4.5. Thus, $^3J_{N\alpha}$ measurements from only the following two data sets are presented: (i) HNHA, pH 4.5, 5 °C, Fab/peptide = 0.0; and (ii) HNHA, pH 4.5, 5 °C, Fab/peptide = 0.3. In addition, although four sets of temperature titrations of $^{15}$N-HSQC spectra were performed (±Fab, pH 7.2 and pH 4.5), only the pH 4.5 data sets were analyzed as the resonances at pH 7.2 rapidly disappeared at temperatures greater than 10 °C, even in the presence of Fab (again due to increased rate of amide proton exchange).

Finally, NOESY and TRNOESY data sets were also acquired at 25 °C, as one might expect the identification of TRNOEs to be easier at higher temperatures due to the attenuation of the free peptide NOEs. However, the TRNOEs (involving both exchangeable and nonexchangeable protons) were observed to develop to greater intensity at 5 °C, a temperature for which all detailed TRNOE analysis were then made. The larger TRNOEs observed at the lower temperature may be due to the fact that a larger population of the peptides are ordered at 5 °C, leading to a larger population of the free peptide already in the "bound conformation". If preorganization of the bound peptide conformation energetically favors binding to antibody, this would lead to a larger proportion of bound peptide and therefore more intense TRNOEs.

*Choice of Fab Concentration Used in NMR Analysis of Bound State.* The limited solubility of the Fab fragment coupled with the large size of the complex (>50 kDa) restricted concentrations to 0.3 mol equiv of Fab/peptide (30% bound population of peptide). Further increases in the concentration of Fab led to marked decreases in the resolution and signal-to-noise of peaks in the $^{15}$N-edited HSQC spectra, precluding the acquisition of interpretable 3D data sets.

Although a 1:1 complex (100% bound population) is ideally preferred for NMR analysis, a 30% bound population in a rapidly exchanging system will still provide information of the bound-state conformation and environment. A 30% contribution from the bound peptide will contribute to a significant change in the measured coupling constant ($^3J_{N\alpha}$) and temperature coefficient ($-\Delta\delta/\Delta T$) if either of these parameters differ substantially between the free and bound states (see eqs 5 and 6 in Results). A 30% contribution from the bound peptide should reflect an even higher bound population in the TRNOESY experiment since the intensity of the TRNOE is dominated by the bound peptide conformation due to the faster cross-relaxation rates of the bound state (see eq 4).

*NMR Spectroscopy.* All 2D and 3D heteronuclear NMR experiments were carried out using the enhanced sensitivity pulsed field gradient method (*32*, *33*) on a Varian Inova-500 or Unity-600 NMR spectrometer equipped with three channels, a pulsed-field gradient triple resonance probe with an actively shielded z gradient, and a gradient amplifier unit. 2D $^{15}$N-HSQC spectra (*34*) were acquired at 600 MHz with the following number of complex points, acquisition times,

[2] NMR structural studies and a full structure calculation of the synthetic PAK pilin peptide were performed at pH 4.5 (*22*). $^1$H NMR-monitored Mab PAK-13 titrations of the synthetic PAK pilin peptide were performed at pH 7.2 (*24*). NMR structural studies of the recombinant $^{15}$N-labeled PAK pilin peptide were performed at pH 4.5 (*26*). $^{15}$N relaxation studies of the recombinant $^{15}$N-labeled PAK pilin peptide in the absence (*31*) and presence (*27*) of Fab were performed at both pH 4.5 and pH 7.2.

Table 1: $^{1}H$ and $^{15}N$ NMR Resonance Assignments for the Trans and Cis Isomers of the Recombinant $^{15}N$-labeled PAK Pilin Peptide

Section A. Trans (pH 4.5, 5 °C)

| residue | $^{15}N$ | NH | αH | βH | γH | δH & others |
|---|---|---|---|---|---|---|
| Lys[128] | | | 4.12 | 1.95 | | |
| Cys[129] | 121.8 | 9.16 | 4.86 | 3.07, 3.29 | | |
| Thr[130] | 116.6 | 8.55 | 4.52 | 4.30 | 1.22 | |
| Ser[131] | 117.3 | 8.54 | 4.52 | 3.84, 3.91 | | |
| Asp[132] | 122.0 | 8.52 | 4.62 | 2.73 | | |
| Gln[133] | 119.7 | 8.36 | 4.26 | 2.00, 2.14 | 2.36 | |
| Asp[134] | 119.9 | 8.41 | 4.61 | 2.74, 2.83 | | |
| Glu[135] | 120.5 | 8.32 | 4.22 | 2.00, 2.09 | 2.36 | |
| Gln[136] | 119.3 | 8.48 | 4.14 | 1.89, 2.15 | | |
| Phe[137] | 118.7 | 8.08 | 4.64 | 3.02, 3.17 | | δ 7.23, ϵ 7.34, ξ 7.29 |
| Ile[138] | 123.7 | 8.07 | 4.38 | 1.82 | 1.11, 1.48<br>0.84 ($\gamma CH_3$) | 0.89 ($\delta CH_3$) |
| Pro[139] | * | * | 4.37 | 1.94, 2.35 | 1.98, 2.10 | 3.63, 3.87 |
| Lys[140] | 121.1 | 8.52 | 4.23 | 1.85 | 1.48 | ϵ 3.00 |
| Gly[141] | 110.1 | 8.65 | 3.91, 4.06 | | | |
| Cys[142] | 118.0 | 8.23 | 4.78 | 3.03, 3.24 | | |
| Ser[143] | 117.5 | 8.48 | 4.49 | 3.89 | | |
| Lys[144] | 123.8 | 8.51 | 4.36 | 1.87 | 1.47 | 1.76, ϵ 3.00 |
| Hs[145] | 127.0 | 8.16 | 4.23 | 1.87, 2.05 | 3.63 | |

Section B. Cis (pH 4.5, 5 °C)

| residue | $^{15}N$ | NH | αH | βH | γH | δH & others |
|---|---|---|---|---|---|---|
| Lys[128] | | | 4.15 | 1.94 | | |
| Cys[129] | 122.2 | 9.02 | 5.06 | 2.96, 3.11 | | |
| Thr[130] | 118.9 | 9.06 | 4.53 | 4.28 | | |
| Ser[131] | 116.6 | 8.47 | 4.58 | 3.60, 3.70 | | |
| Asp[132] | 122.5 | 8.52 | 4.62 | 2.67, 2.82 | | |
| Gln[133] | 118.8 | 8.31 | 4.20 | 2.05 | 2.34 | |
| Asp[134] | 119.7 | 8.36 | 4.62 | | | |
| Glu[135] | 116.5 | 8.29 | 4.05 | | | |
| Gln[136] | 118.8 | 8.08 | 4.30 | 1.95 | | |
| Phe[137] | 121.0 | 8.27 | | 2.97, 3.17 | | |
| Ile[138] | 121.8 | 8.39 | 4.37 | | | |
| Pro[139] | * | * | 4.72 | 2.11, 2.41 | | |
| Lys[140] | 121.8 | 8.67 | 4.25 | 1.85 | | |
| Gly[141] | 112.5 | 8.91 | 3.87, 4.14 | | | |
| Cys[142] | 118.0 | 8.35 | 4.56 | 3.16, 3.27 | | |
| Ser[143] | 116.9 | 8.43 | 4.41 | 3.63, 3.70 | | |
| Lys[144] | 124.1 | 8.36 | 4.24 | 1.86 | | 1.71, ϵ 3.00 |
| Hs[145] | 126.2 | 8.04 | | | | |

Section C. Trans (pH 7.2, 5 °C)

| residue | $^{15}N$ | NH | residue | $^{15}N$ | NH |
|---|---|---|---|---|---|
| Lys[128] | | | Phe[137] | 119.3 | 8.13 |
| Cys[129] | | | Ile[138] | 123.8 | 8.03 |
| Thr[130] | 116.5 | 8.53 | Pro[139] | * | * |
| Ser[131] | 117.4 | 8.55 | Lys[140] | 121.3 | 8.53 |
| Asp[132] | 122.6 | 8.54 | Gly[141] | 110.2 | 8.66 |
| Gln[133] | 119.6 | 8.29 | Cys[142] | 118.2 | 8.25 |
| Asp[134] | 120.8 | 8.39 | Ser[143] | 117.8 | 8.50 |
| Glu[135] | 121.5 | 8.47 | Lys[144] | 124.2 | 8.52 |
| Gln[136] | 119.3 | 8.52 | Hs[145] | 127.5 | 8.15 |

Section D. Cis (pH 7.2, 5 °C)

| residue | $^{15}N$ | NH | residue | $^{15}N$ | NH |
|---|---|---|---|---|---|
| Lys[128] | | | Phe[137] | 121.3 | 8.23 |
| Cys[129] | | | Ile[138] | 122.1 | 8.29 |
| Thr[130] | 118.7 | 8.99 | Pro[139] | * | * |
| Ser[131] | 116.8 | 8.48 | Lys[140] | 122.0 | 8.67 |
| Asp[132] | 122.9 | 8.53 | Gly[141] | 112.5 | 8.92 |
| Gln[133] | 118.8 | 8.26 | Cys[142] | 118.3 | 8.39 |
| Asp[134] | 120.5 | 8.36 | Ser[143] | 117.1 | 8.46 |
| Glu[135] | 118.1 | 8.38 | Lys[144] | 124.4 | 8.39 |
| Gln[136] | 118.7 | 8.18 | Hs[145] | 126.8 | 8.05 |

and spectral widths: F1 ($^{15}N$) 256, 85 ms, 1500 Hz; F2 ($^{1}H$) 1024, 78 ms, 6600 Hz; 8 transients. 3D $^{15}N$-edited HSQC NOESY and $^{15}N$-edited HSQC TRNOESY (*34*, *35*) experiments were performed at 600 MHz and at mixing times of 150 and 300 ms with the following number of complex points, acquisition times, and spectral widths: F1 ($^{1}HN$) 240, 24 ms, 5000 Hz; F2 ($^{1}H$) 1024, 78 ms, 6600 Hz; F3 ($^{15}N$) 52, 21 ms, 1217 Hz; 12 transients. HNHA experiments (*36*)

were performed at 500 MHz and employed the following number of complex points, acquisition times, and spectral widths: F1 ($^1$HN) 112, 16 ms, 3500 Hz; F2 ($^1$H) 768, 64 ms, 6000 Hz; F3 ($^{15}$N) 64, 32 ms, 1000 Hz; 16 transients.

*Data Processing and Analysis.* All 2D and 3D data sets were processed on SUN Sparc5 and Silicon Graphics Indigo2 workstations using NMRPipe and NMRDraw software provided by F. Delaglio (NIDDK, NIH, Gaithersburg, MD, unpublished). Spectra assignment was achieved using the interactive graphic-based program PIPP (*37*). Post-acquisition solvent subtraction was employed in the spectra where backbone amide protons were detected in the acquisition dimension (*38*). Typically, spectra were processed in the acquisition and indirect dimension with 90° shifted sine-bell squared apodization. For constant time $^{15}$N evolution periods, mirror image linear prediction was used to double the time domain signals (*39*). A time domain deconvolution procedure (*33*) was used to minimize the signal from residual water for $^{15}$N-edited 3D experiments.

Temperature coefficients ($-\Delta\delta/\Delta T$) were calculated for the amide protons of recombinant PAK pilin from linear plots of chemical shift versus temperature measured from $^{15}$N-HSQC spectra acquired at 5, 10, 15, and 20, and 25 °C. $^3J_{N\alpha}$ coupling constants were obtained for each residue from the ratio of the intensities of the diagonal peak of residue *i* to its $\alpha$H$-$NH(*i*,*i*) cross-peak in the HNHA spectra (*36*).

*Theory of the Transferred Nuclear Overhauser Effect.* The transferred nuclear Overhauser effect (TRNOE) is an extension of the nuclear Overhauser effect (NOE) to exchanging systems such as peptide$-$protein complexes (*40*). In the present study, a 3D $^{15}$N-edited HSQC TRNOESY experiment is used to measure the intensity of the TRNOE. Although the theory outlined below is developed for the 2D TRNOESY experiment, the equations are easily adapted to the 3D $^{15}$N-edited HSQC TRNOESY as the third $^{15}$N dimension (F2) merely serves to edit the $^1$H$-^1$H TRNOESY in the F1$-$F3 plane according to the $^{15}$N chemical shift of the backbone amide.

In the presence of chemical exchange, NOEs conveying conformational information of the bound peptide are "transferred" to the free peptide resonances where they are more easily measured because these resonances are much narrower. The only necessary condition for the transfer of magnetization is that the exchange rate be faster than the $T_1$ longitudinal relaxation rate of the bound peptide ($k_{-1} > 1/T_{1B}$). Equation 1 diagramatically represents a system undergoing chemical exchange, in this case the recombinant PAK pilin peptide binding to Fab PAK-13. Here, $P_F$ and $P_B$ are the free and bound peptide, $k_1$[Fab] and $k_{-1}$ are the exchange rates, $\tau_{ijF}$ and $\tau_{ijB}$ are the correlation times that modulate the interaction between protons *i* and *j* in the free and bound peptide, and $W_{ijF}$ and $W_{ijB}$ are the dipolar cross-relaxation rates between protons *i* and *j* in the free and bound peptide (proportional to the measured NOE intensities, $NOE_{ijF}$ and $NOE_{ijB}$, at short mixing times):

$$\begin{array}{ccc} \text{Fab} + P_F & \underset{k_{-1}}{\overset{k_1[\text{Fab}]}{\rightleftharpoons}} & \text{Fab}\cdot P_B \\ \tau_{ijF} \approx 10^{-9}\,\text{s} & & \tau_{ijB} > 10^{-9}\,\text{s} \\ W_{ijF} \propto \text{NOE}_{ijF} & & W_{ijB} \propto \text{NOE}_{ijB} \end{array} \quad (1)$$

In the presence of fast exchange on the NMR time scale,[3] the observed chemical shifts, $\delta_{obs}$, and line widths, $\Delta\nu_{obs}$, are dominated by the free peptide population when $P_F > P_B$:

$$\delta_{obs} = P_B\delta_B + P_F\delta_F \quad (2)$$

$$\Delta\nu_{obs} = P_B\Delta\nu_B + P_F\Delta\nu_F \quad (3)$$

Conversely, the intensity of the TRNOE is dominated by the bound peptide conformation (even for $P_F > P_B$), since the cross-relaxation rates for the bound peptide are so much faster than they are for the free ($W_{ijB} \gg W_{ijF}$):

$$\text{TRNOE}_{ij} \propto -[P_B W_{ijB} + P_F W_{ijF}] \cong P_B W_{ijB} \cong P_B \text{NOE}_{ijB} \quad (4)$$

Thus, $^1$H$-^1$H TRNOE cross-peak intensities measured in the F1$-$F3 plane of the $^{15}$N-edited HSQC TRNOESY experiment will provide interproton distances for the bound peptide ($NOE_{ijB} \propto r_{ijB}^{-6}$) in much the same way that NOE cross-peak intensities provide interproton distances for the free state ($NOE_{ijF} \propto r_{ijF}^{-6}$).

## RESULTS

*Determination of the Exchange Regime for the PAK Pilin Peptide-Fab PAK-13 Complex.* The exchange regime for the PAK pilin peptide-Fab PAK-13 complex was determined using a combination of competitive ELISA experiments and chemical shift analysis. Competitive ELISA experiments were performed at pH 7.2 and produced a $K_a$ of $6.3 \pm 0.5 \times 10^6$ M$^{-1}$ for the binding of the recombinant PAK pilin peptide to Mab PAK-13.[4] For $K_a = k_1$[Fab]$/k_{-1}$ and assuming that $k_1$[Fab] $= 10^8$ M$^{-1}$ s$^{-1}$ (the diffusion controlled rate), $k_{-1}$ is calculated to be on the order of 100 s$^{-1}$. Chemical shift perturbations observed for the PAK pilin peptide trans and cis resonances as a function of added Fab PAK-13 provide a second independent measure of $k_{-1}$. Taking the perturbation of 0.09 ppm measured for the trans Cys$^{142}$ NH resonance at an Fab/peptide molar equivalent of 0.3 ($P_B = 0.3$), pH 7.2 (see next section), we can estimate the total chemical shift separation ($\Delta\delta = |\delta_F - \delta_B|$) to be 0.3 ppm, equivalent to 150 Hz at a field of 500 MHz. From the definition of fast exchange on the chemical shift time scale given in footnote 3, $k_{-1}$ is calculated be greater than 105 s$^{-1}$ at pH 7.2 for the trans isomer.[5] Similarily, using the perturbation of 0.12 ppm measured at $P_B = 0.3$, pH 7.2, for

[3] Fast exchange on the chemical shift time scale is defined as $k_{-1}(1 + P_B/P_F) \gg \Delta\delta$ where $\Delta\delta = |\delta_F - \delta_B|$, the chemical shift separation of the resonances of the free and bound ligand. Fast exchange on the relaxation time scale is defined as $k_{-1}(1 + P_B/P_F) \gg \Delta T_2$ where $\Delta T_2 = |T_{2F} - T_{2B}|$, the difference in the transverse relaxation times of the free and bound ligand (*41*).

[4] Competitive ELISA experiments of the synthetic PAK pilin peptide binding to Mab PAK-13 produced a $K_a$ of $10.3 \pm 1.0 \times 10^6$ M$^{-1}$. No competitive ELISA experiments for either the synthetic or recombinant pilin peptide were performed at pH 4.5, as the pH dependence of the interaction between Mab PAK-13 and the goat anti-mouse IgG immunoglobulin conjugated to horseradish peroxidase is unknown and introduces an indeterminate variable into the measurement.

[5] Estimation of $k_{-1}$ from chemical shift analysis only yields a lower limit for the off-rate. A more direct measure of $k_{-1}$ from surface plasmon resonance measurements on a BIAcore biosensor was attempted but yielded $k_{-1}$ too fast for measurement.

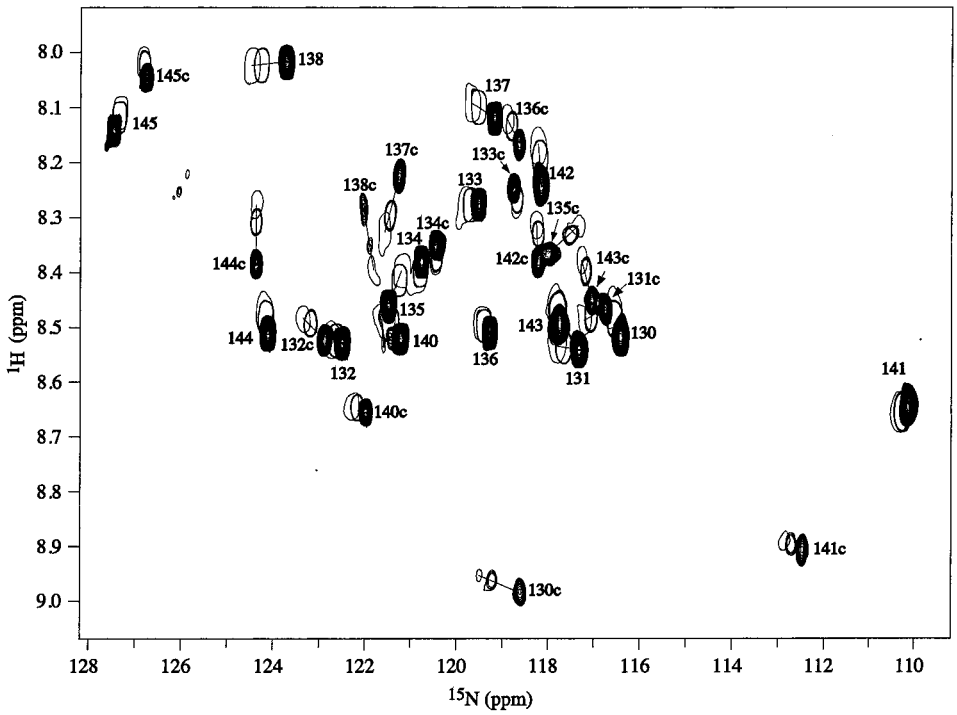


FIGURE 1: Superimposed 2D $^{15}$N-HSQC spectra of recombinant $^{15}$N-labeled PAK pilin peptide titrated with Fab PAK-13. Three different steps are shown with Fab/peptide molar equivalents of 0.0 (multiple contours), 0.15 (three contours), and 0.3 (single contour). A doubling of resonances is observed for each peak due to cis/trans isomerization around the central Ile$^{138}$-Pro$^{139}$ peptide bond. Peaks arising from the minor cis isomer are denoted by the subscript c after the residue, i.e., 144c, to differentiate them from the major trans peaks. The original peptide sample was 1 mM in PBS buffer, pH 7.2, and 90% $H_2O$/10% $D_2O$ at 5.0 °C.

the cis Ile$^{138}$ NH resonance (see also next section), $k_{-1}$ is calculated to be greater than 140 $s^{-1}$ for the cis isomer. The off-rates calculated for the binding of the trans and cis isomers to Fab PAK-13 are similar to each other and are of the same order of magnitude as that obtained from the competitive ELISA binding measurements for binding to the intact IgG. An off-rate of $k_{-1} \gg 100$ $s^{-1}$ is consistent with the observation of a single set of trans and cis peptide resonances throughout the antibody titration, with a "weighted average" chemical shift and line width determined by the populations of free and bound isomers.

*Chemical Shift Perturbation Mapping.* A conceptually simple but effective technique for mapping binding surfaces by NMR uses chemical shift perturbation mapping (*42*−*44*). This technique involves monitoring changes in chemical shift as a function of added titrant and requires that the system be in fast exchange on the chemical shift time scale (see footnote 3). Chemical shift perturbations were used to map the PAK-13 binding surface on the recombinant PAK pilin peptide. Figure 1 shows the $^{15}$N-HSQC titration at pH 7.2 of the recombinant $^{15}$N-labeled PAK pilin peptide with Fab PAK-13, where the different steps correspond to Fab/peptide mol equiv of 0.0 (multiple contours), 0.15 (three contours), and 0.3 (single contour). The doubling of peaks arises from isomerization around the central Ile$^{138}$-Pro$^{139}$ peptide bond, which produces a major trans isomer and a minor cis isomer at a ratio of approximately 5:1 trans/cis (5 °C). The energy barrier of $\Delta G^{\ddagger} \approx 20$ kcal/mol for cis/trans interconversion of peptide groups (*45*−*47*) makes this conformational exchange rate relatively slow ($<1$ $s^{-1}$), much slower than the off-rate of the peptide from the antibody molecule ($10^2$ $s^{-1}$ at pH 7.2). Thus, the observation of chemical shift perturbations of similar magnitude for both the trans and cis resonances in the titration indicates that each isomer binds directly to the antibody, with apparently similar affinity. This may be due to the presence in both isomers of the second $\beta$-turn spanning Pro$^{139}$-Lys-Gly-Cys$^{142}$, which has been identified as part of the structural epitope for PAK-13 binding from previous $^1$H NMR studies (*24*).

A $^{15}$N-HSQC titration of the recombinant $^{15}$N-labeled PAK pilin peptide with Fab PAK-13 was also performed at pH 4.5 using the same molar equivalents for each step in the titration (data not shown). The titration at pH 4.5 showed a similar pattern of perturbations for the trans and cis resonances but with final shifts (Fab/peptide = 0.3) on the average of 10−15% smaller in magnitude than those observed at pH 7.2. This suggests that the $K_a$ for each isomer at pH 4.5 is slightly smaller than that at pH 7.2, although still within the same order of magnitude ($10^6$−$10^7$ $M^{-1}$).

Chemical shift perturbations were directly measured from the $^{15}$N-HSQC titrations of the recombinant $^{15}$N-labeled PAK pilin peptide with Fab PAK-13 and are plotted by residue in Figure 2 (trans isomer) and Figure 3 (cis isomer). Figures 2A−C and 3A−C show $^{15}$N, NH, and averaged backbone perturbations measured at pH 7.2 for trans and cis resonances, respectively, taken directly from the HSQC data plotted in Figure 1. Figures 2D−H and 3D−H show $^{15}$N, NH, αH, averaged backbone, and side chain perturbations measured at pH 4.5 for trans and cis resonances, respectively. The backbone αH and side chain $\beta$H and $\gamma$H perturbations measured at pH 4.5 are taken from the $^{15}$N-edited HSQC NOESY and TRNOESY spectra plotted in Figures 4 and 5.

The chemical shift perturbations observed for trans isomer of the recombinant PAK pilin peptide are similar at pH 7.2 (Figure 2A,B) versus pH 4.5 (Figure 2D,E), both in terms

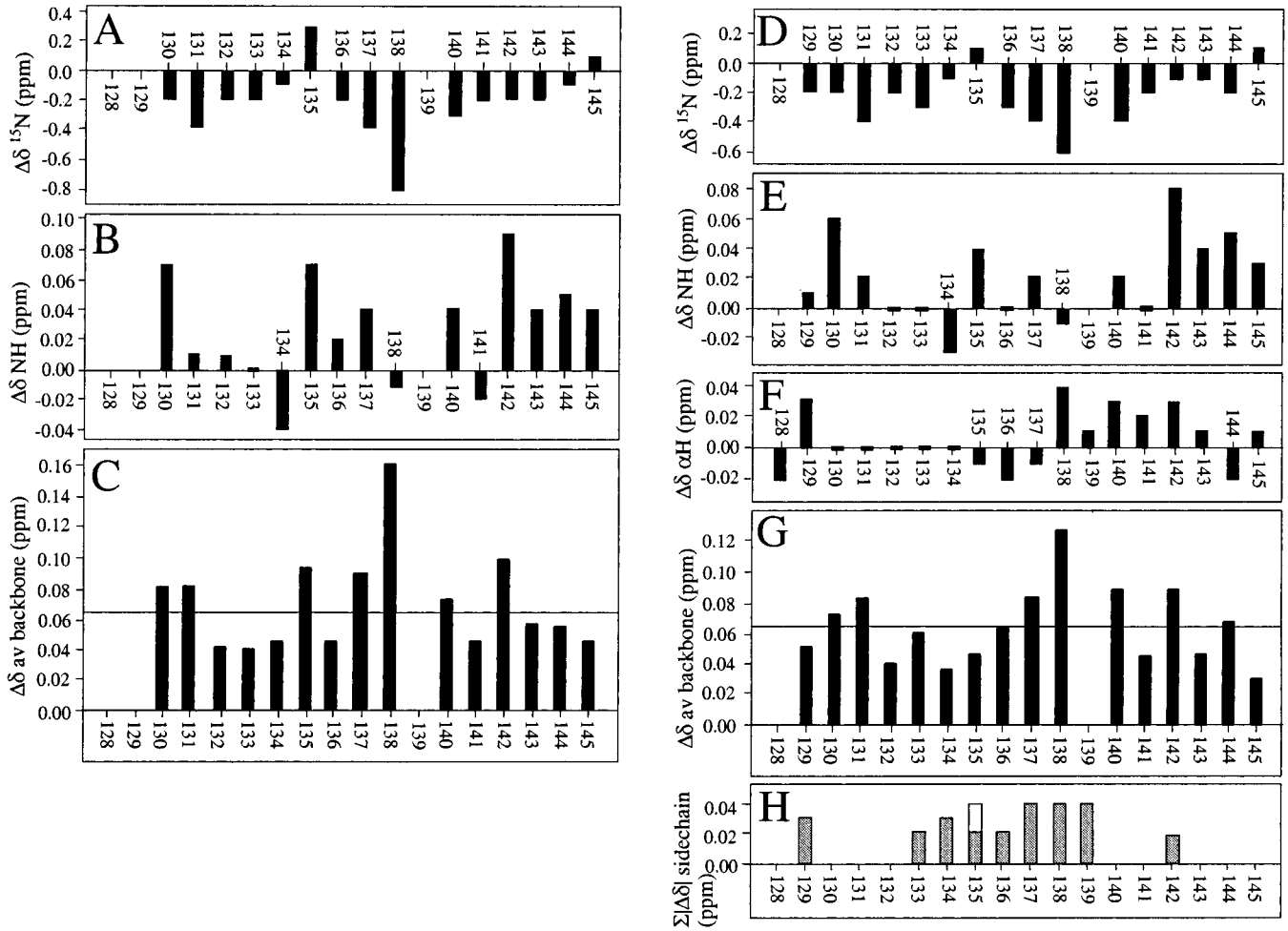


FIGURE 2: Chemical shift perturbations observed in the Fab PAK-13 titrations of the trans isomer of recombinant $^{15}$N-labeled PAK pilin peptide performed at pH 7.2 and pH 4.5. The left panels (A−C) show $^{15}$N ($\Delta\delta^{15}$N), NH ($\Delta\delta$NH), and averaged backbone ($\Delta\delta$av = $\{(\Delta\delta^{15}\text{N})^2 + (\Delta\delta\text{NH})^2\}^{1/2}$) perturbations measured at pH 7.2 from the HSQC data plotted in Figure 1. The right panels (D−H) show $^{15}$N ($\Delta\delta^{15}$N), NH ($\Delta\delta$NH), αH ($\Delta\delta\alpha$H), averaged backbone ($\Delta\delta\text{av} = \{(\Delta\delta^{15}\text{N})^2 + (\Delta\delta\text{NH})^2 + (\Delta\delta\alpha\text{H})^2\}^{1/2}$), and side chain ($\Sigma|\Delta\delta|$) perturbations measured at pH 4.5 from the $^{15}$N-edited HSQC NOESY spectra plotted in Figure 4. The horizontal line in panels C and G corresponds to the average deviation. Each perturbation corresponds to the chemical shift measured at 0.3 mol equiv of Fab/peptide (values are not extrapolated to a 1:1 complex). Backbone perturbations, $\Delta\delta$, were calculated as $[\Delta\delta = \delta_{(-\text{Fab})} - \delta_{(+\text{Fab})}]$, such that an upfield shift in the presence of Fab is indicated by a positive $\Delta\delta$. Side chain perturbations were calculated as the sum of all observed shifts ($\Sigma|\Delta\delta| = |\Delta\delta\beta\text{H}| + |\Delta\delta\gamma\text{H}|$), using the absolute value of each shift. The gray and white shadings represent $|\Delta\delta\beta\text{H}|$ and $|\Delta\delta\gamma\text{H}|$, respectively.

of the direction of the perturbations (downfield versus upfield) and in terms of the relative magnitudes of the perturbations. For example, the amide $^{15}$N of Ile$^{138}$ displays the greatest downfield perturbation, and the amide proton of Cys$^{142}$ displays the greatest upfield perturbation, regardless of pH. As chemical shifts are exquisitely sensitive to their local electronic environment, the similarity of the perturbations at pH 7.2 versus pH 4.5 indicates that a change in pH is not significantly changing the antibody binding surface on the trans isomer. This is an important initial result as it suggests that pH changes in the range of 4.5−7.2 do not significantly affect either peptide conformation or antibody recognition. Thus, the results of all experiments performed within this pH range should present a consistent picture of antibody binding.

Whereas the individual $^{15}$N and NH perturbations suggest similar antibody binding surfaces at pH 7.2 versus 4.5, these individual perturbations are not easily interpreted. However, by summing and averaging all measurable backbone perturbations on a per residue basis, a consistent map of the "binding surface" can emerge (*44*). Averaged backbone perturbations were calculated for the trans isomer as $\Delta\delta_{\text{av}} = \{(\Delta\delta^{15}\text{N})^2 + (\Delta\delta\text{NH})^2\}^{1/2}$ at pH 7.2 and $\Delta\delta_{\text{av}} = \{(\Delta\delta^{15}\text{N})^2 + (\Delta\delta\text{NH})^2 + (\Delta\delta\alpha\text{H})^2\}^{1/2}$ at pH 4.5, where the αH shifts at pH 4.5 were measured from $^{15}$N-edited HSQC NOESY and TRNOESY spectra. As expected, the plots of $\Delta\delta_{\text{av}}$ versus sequence at pH 7.2 (Figure 2C) and pH 4.5 (Figure 2G) are very similar. For example, both plots show $\Delta\delta_{\text{av}}$ to be significantly greater than the mean for Thr$^{130}$ and Ser$^{131}$ in the N-terminal half of the peptide, Phe$^{137}$ at the end of the first turn, Ile$^{138}$ between the turns, and Cys$^{142}$ at the end of the second turn. The only obvious pH-related difference between the plots is that $\Delta\delta_{\text{av}}$ for Glu$^{135}$ is significantly greater at pH 7.2 ($\Delta\delta_{\text{av}}$ = 0.09 ppm at pH 7.2 versus 0.05 ppm at pH 4.5). This difference could be attributed to the titration of the Glu$^{135}$ glutamyl side chain[6] within the pH 4.5−7.2 range.

[6] A $^1$H NMR-monitored pH titration of the synthetic PAK pilin peptide showed titration of the backbone amide resonance of Glu$^{135}$ from 8.25 ppm at pH 4 to 8.48 ppm at pH 8, with a p$K_a$ of approximately 4.5. No other residues displayed significant chemical shifts within this pH range.

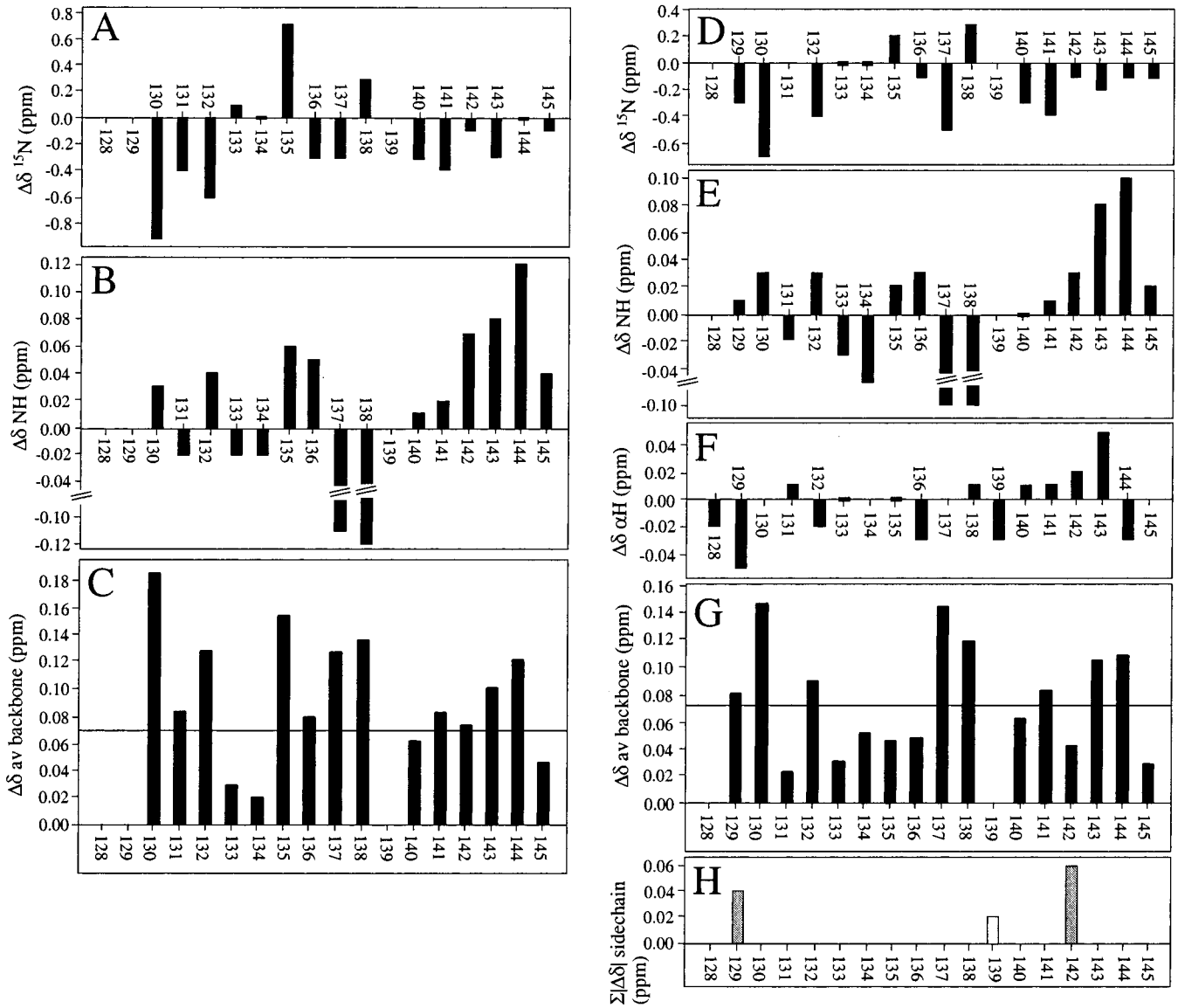


FIGURE 3: Chemical shift perturbations observed in the Fab PAK-13 titrations of the cis isomer of recombinant $^{15}$N-labeled PAK pilin peptide performed at pH 7.2 and pH 4.5. The left panels (A−C) show $^{15}$N ($\Delta\delta^{15}$N), NH ($\Delta\delta$NH), and averaged backbone ($\Delta\delta_{av} = \{(\Delta\delta^{15}N)^2 + (\Delta\delta NH)^2\}^{1/2}$) perturbations measured at pH 7.2 from the HSQC data plotted in Figure 1. The right panels (D−H) show $^{15}$N ($\Delta\delta^{15}$N), NH ($\Delta\delta$NH), αH ($\Delta\delta\alpha$H), averaged backbone ($\Delta\delta_{av} = \{(\Delta\delta^{15}N)^2 + (\Delta\delta NH)^2 + (\Delta\delta\alpha H)^2\}^{1/2}$), and side chain ($\Sigma|\Delta\delta|$) perturbations measured at pH 4.5 from the $^{15}$N-edited HSQC NOESY spectra plotted in Figure 5. For definitions of perturbations and symbols, refer to the legend of Figure 2.

The chemical shift perturbations observed for cis isomer of the recombinant PAK pilin peptide (Figure 3) are also similar at pH 7.2 versus pH 4.5; large NH perturbations are observed for Phe$^{137}$, Ile$^{138}$, and Lys$^{144}$ at both pH values. This indicates that a change in pH does not significantly change the antibody binding surface on the cis isomer. Again, the only significant pH-related difference is associated with Glu$^{135}$, which displays one of the greatest perturbations at pH 7.2 ($\Delta\delta_{av} = 0.15$ ppm) as compared to one of the smallest perturbations at pH 4.5 ($\Delta\delta_{av} = 0.04$ ppm). Interestingly, the residues associated with the greatest $\Delta\delta_{av}$ in the cis isomer (Thr$^{130}$, Asp$^{132}$, Phe$^{137}$, Ile$^{138}$, Lys$^{144}$, and Hs$^{145}$) are not exactly the same as those in the trans isomer (Thr$^{130}$, Ser$^{131}$, Phe$^{137}$, Ile$^{138}$, and Cys$^{142}$). Thus, the trans and cis isomers appear to "expose" different surfaces to antibody binding.

What do these patterns of perturbations mean, and are they correlated to actual contact surfaces on the 3D and solution structures of the trans and cis isomers, or do they correspond to regions that are undergoing subtle changes in either conformation or dynamics? The NMR solution structure of the trans isomer of the synthetic PAK pilin peptide (*22*) shows that the backbone segments spanned by Thr$^{130}$-Ser$^{131}$ and Phe$^{137}$-Ile$^{138}$ are on opposite faces of the peptide. Therefore, the chemical shift perturbation map of the trans isomer cannot correspond to an actual continuous surface. However, $^{15}$N NMR relaxation experiments made of the trans isomer of the recombinant $^{15}$N-labeled PAK pilin peptide in the absence of Fab (*31*) detected exchange processes on the microsecond to millisecond time scale for Thr$^{130}$, Gln$^{136}$, Phe$^{137}$, Ile$^{138}$, and Lys$^{140}$ at pH 4.5 and for Thr$^{130}$, Glu$^{135}$, Gln$^{136}$, Phe$^{137}$, Ile$^{138}$, and Lys$^{140}$ at pH 7.2. Interestingly, the amplitude of these motions "peaked" around Ile$^{138}$ at both pH values, as did the magnitude of the backbone perturbations. Thus, the chemical shift perturbation map of the trans isomer does appear to coincide with regions of the backbone

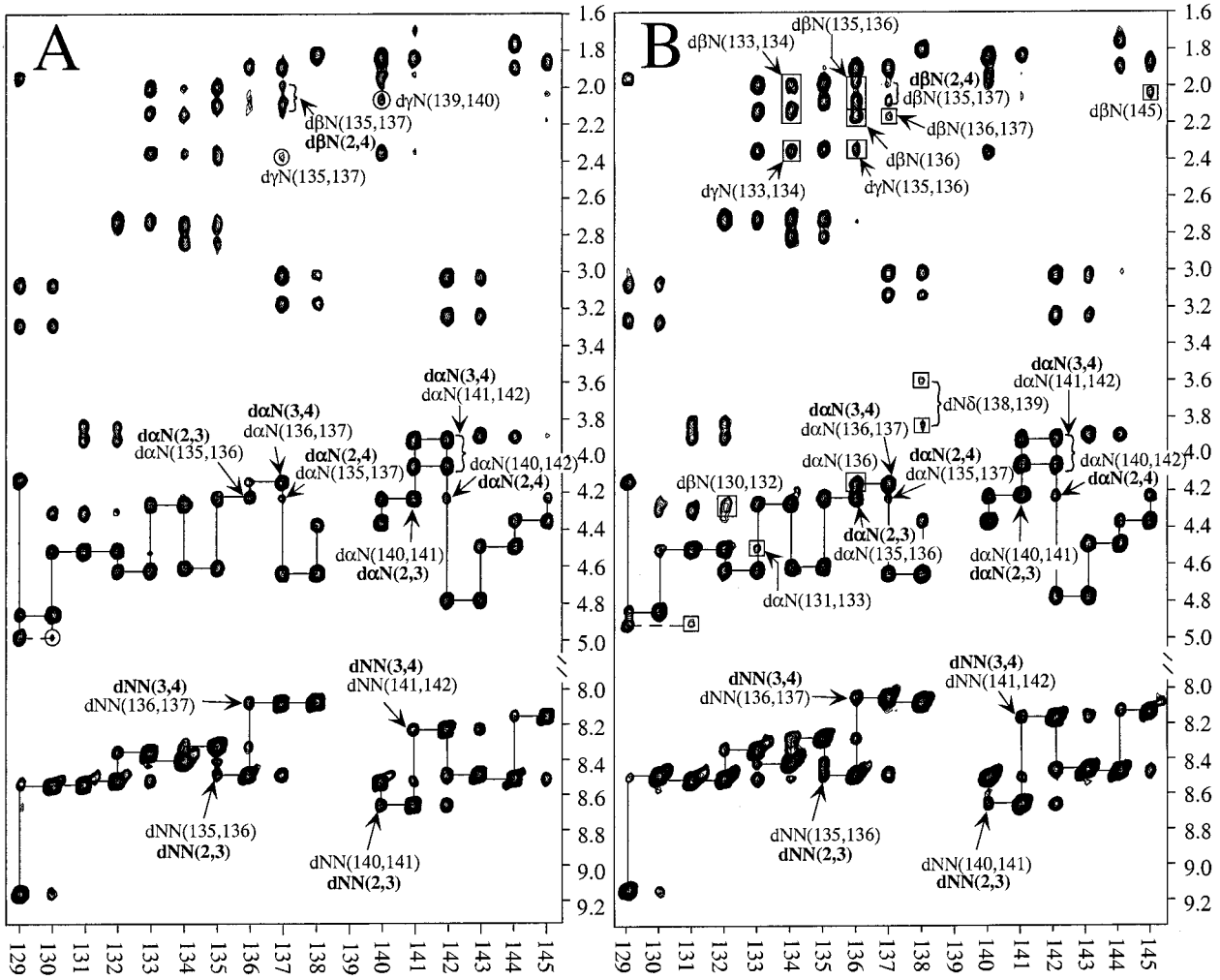


FIGURE 4: Strip plots from the 3D $^{15}$N-edited HSQC NOESY spectrum of the trans isomer of recombinant $^{15}$N-labeled PAK pilin peptide in the absence and presence of Fab PAK-13. Panel A shows NOEs in the absence of Fab, whereas panel B shows TRNOEs in the presence of 0.3 mol equiv of Fab/peptide. Circled NOEs in panel A diminish significantly in intensity in the presence of Fab. Boxed TRNOEs in panel B develop significantly in intensity in the presence of Fab. NOEs and TRNOEs identifying the $\beta$-turns spanned by residues Asp$^{134}$-Glu-Gln-Phe$^{137}$ and Pro$^{139}$-Lys-Gly-Cys$^{142}$ in the trans isomer are identified as $d_{\alpha N}(2,3)$, $d_{\alpha N}(3,4)$, $d_{\alpha N}(2,4)$, $d_{\beta N}(2,4)$, $d_{NN}(2,3)$, and $d_{NN}(3,4)$, where the number indicates the position in each turn. The original peptide sample was 1 mM in PBS buffer, pH 4.5, and 90% $H_2O$/10% $D_2O$ at 5.0 °C. The final peptide sample with Fab was 1 mM peptide, 0.30 mM Fab PAK-13, PBS buffer, pH 4.5, and 90% $H_2O$/10% $D_2O$ at 5.0 °C.

that undergo slow microsecond to millisecond "exchange-related" motions. These motions may play a role in induced fit binding to Mab PAK-13, which would allow the same antibody combining site to accommodate two different binding topologies (trans versus cis isomer, for example). To resolve some of these dynamical issues, we have performed $^{15}$N NMR relaxation studies of the $^{15}$N-labeled recombinant PAK pilin peptide in complex with Fab PAK-13. The results of these studies will be presented in a forthcoming paper (*27*).

Finally, side chain chemical shift perturbations were measured for the trans and cis isomers at pH 4.5 only and are plotted in panel H of Figures 2 (trans isomer) and 3 (cis isomer). The trans isomer displays side chain perturbations for the disulfide bridge (Cys$^{129}$-Cys$^{142}$) as well as for the stretch of sequence spanned by Gln$^{133}$-Asp$^{134}$-Glu$^{135}$-Gln$^{136}$-Phe$^{137}$-Ile$^{138}$-Pro$^{139}$. Interestingly, these residues do present a solid continuous surface, which represents roughly half of the peptide (*22*) and includes the first turn (Asp$^{134}$-Glu$^{135}$-Gln$^{136}$-Phe$^{137}$) and the hydrophobic pocket (Phe$^{137}$, Ile$^{138}$, Pro$^{139}$). Unfortunately, the poor signal-to-noise associated with the cis isomer prohibited measurement of most side chain perturbations, although side chain perturbations for the disulfide bridge are observed. Clearly, $^{13}$C-edited NMR studies of a $^{13}$C-labeled recombinant PAK pilin peptide free in solution versus in complex with Fab PAK-13 are required to further probe antibody-induced changes in side chain conformation and dynamics.

*TRNOESY Experiments.* We next performed TRNOESY experiments of the recombinant $^{15}$N-labeled PAK pilin peptide bound to Fab PAK-13. These experiments should allow us to determine if backbone perturbations are also related to changes in peptide backbone conformation induced by Fab binding. In an earlier study, a 2D homonuclear TRNOESY was used to probe for conformational changes in the unlabeled synthetic PAK pilin peptide bound to the same antibody fragment (*24*). However, the interpretation of these experiments was limited by the spectral overlap of several key connectivities, especially in the case of the less intense cis resonances. In the present study, the 3D $^{15}$N-edited HSQC NOESY pulse sequence is used to perform a $^{15}$N-edited HSQC TRNOESY. Spectral editing in the F2 dimen-

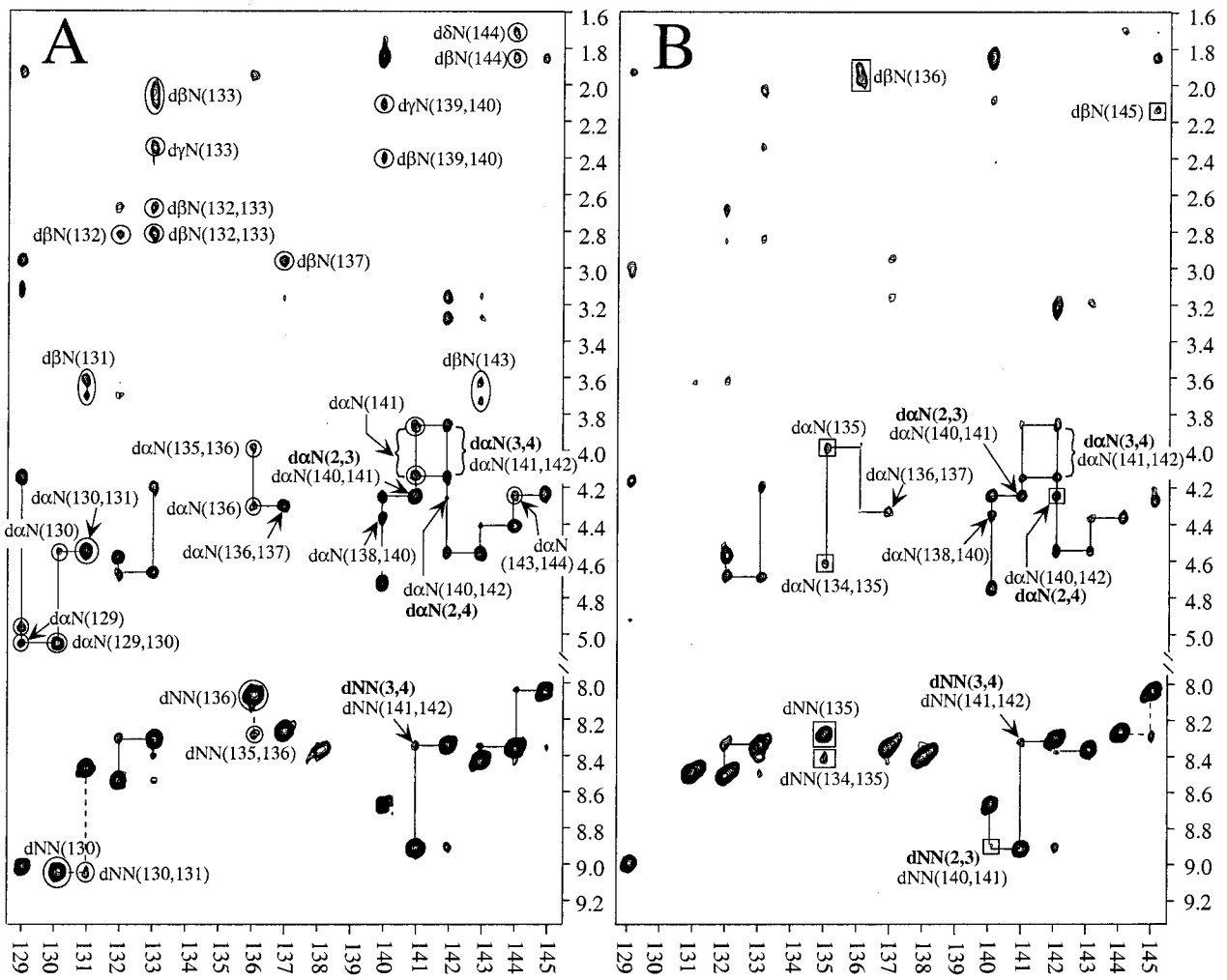


FIGURE 5: Strip plots from the 3D $^{15}$N-edited HSQC NOESY spectrum of the cis isomer of recombinant $^{15}$N-labeled PAK pilin peptide in the absence and presence of Fab PAK-13. Panel A shows NOEs in the absence of Fab, whereas panel B shows TRNOEs in the presence of 0.3 mol equiv of Fab/peptide. Circled NOEs in panel A diminish significantly in intensity in the presence of Fab. Boxed TRNOEs in panel B develop significantly in intensity in the presence of Fab. NOEs and TRNOEs identifying the $\beta$-turn spanned by residues Pro$^{139}$-Lys-Gly-Cys$^{142}$ are identified as $d_{\alpha N}(2,3)$, $d_{\alpha N}(3,4)$, $d_{\alpha N}(2,4)$, $d_{\beta N}(2,4)$, $d_{NN}(2,3)$, and $d_{NN}(3,4)$, where the number indicates the position in the turn. Sample conditions are described in the legend for Figure 4.

sion according to the $^{15}$N chemical shift of the backbone amide should resolve overlap issues and allow the bound conformation of the cis isomer to be detected.

$^{15}$N-edited HSQC TRNOESYs were performed at both pH 4.5 and pH 7.2. The experiment at pH 7.2 displayed poor signal-to-noise, presumably due to an increased rate of base-catalyzed exchange of amide protons with bulk water. Thus, only the pH 4.5 data are presented and discussed in the manuscript. However, it should be noted that the pattern of backbone connectivities observed in the absence and presence of Fab was the same at either pH. Thus, conclusions drawn from the pH 4.5 data are assumed to be valid within the pH range of 4.5−7.2. This assumption is supported by the similarity of the chemical shift perturbations observed in the Fab titrations performed at pH 4.5 versus pH 7.2.

Figures 4 and 5 show strip plots extracted from the 300 ms mixing time $^{15}$N-edited HSQC NOESY and TRNOESY spectra of the trans (Figure 4) and cis (Figure 5) isomers of the recombinant $^{15}$N-labeled PAK pilin peptide in the absence and presence of 0.3 mol equiv of Fab PAK-13 (at pH 4.5). In the absence of Fab, the trans isomer displays strong $d_{NN}(136,137)$ and $d_{NN}(141,142)$ and medium and weak $d_{\alpha N}(135,137)$ and $d_{\alpha N}(140,142)$ connectivities (Figure 4A). These NOEs are diagnostic of two $\beta$-turns in the regions Asp$^{134}$-Glu-Gln-Phe$^{137}$ and Pro$^{139}$-Lys-Gly-Cys$^{142}$ (*26*).[7] A predominant type II configuration for the turn spanning Pro$^{139}$-Lys-Gly-Cys$^{142}$ is suggested by a strong $d_{\alpha N}(140,141)$ versus medium $d_{NN}(140,141)$ connectivity and by the absence of any $d_{\beta N}(140,142)$ connectivity. A predominant type I configuration for the turn spanning Asp$^{134}$-Glu-Gln-Phe$^{137}$ is suggested by a medium $d_{\alpha N}(135,136)$ connectivity and the existence of a moderately strong $d_{\beta N}(135,137)$ connectivity. In the absence of Fab, the cis isomer displays a moderate

[7] The NOEs diagnostic of $\beta$-turns include $d_{\alpha N}(2,3)$, $d_{\alpha N}(3,4)$, $d_{\alpha N}(2,4)$, $d_{NN}(2,3)$, and $d_{NN}(3,4)$ cross-peaks (*48*, *49*) where the numbering indicates the position in the turn. The NOEs required for positive identification of a $\beta$-turn are a weak $d_{\alpha N}(2,4)$ cross-peak, corresponding to a distance of 3.6 Å in the type I turn and 3.3 Å in the type II turn, and a strong $d_{NN}(3,4)$ cross-peak, corresponding to a distance of 2.4 Å in both types of turns. Type I and type II turns may be distinguished by the relative strengths of the $d_{\alpha N}(2,3)$ and the $d_{NN}(2,3)$ cross-peaks. The type I turn displays a medium $d_{\alpha N}(2,3)$ cross-peak and a strong $d_{NN}(2,3)$ cross-peak, corresponding to distances of 3.4 and 2.6 Å, respectively; whereas the type II turn displays a strong $d_{\alpha N}(2,3)$ cross-peak and a weak $d_{NN}(2,3)$ cross-peak, where the corresponding distances are 2.2 and 4.5 Å. In addition, the $d_{\beta N}(2,4)$ cross-peak is moderately strong for a type I turn since this distance can approach as closely as 2.9 Å in a type I turn but only as close as 3.6 Å in a type II turn.

$d_{NN}$(141,142) and a weak $d_{\alpha N}$(140,142) connectivity (Figure 5A), diagnostic of a single $\beta$-turn spanning Pro[139]-Lys-Gly-Cys[142]. The existence of a strong $d_{\alpha N}$(140,141) versus a weak $d_{NN}$(140,141) connectivity coupled with the absence of any $d_{\beta N}$(140,142) connectivity suggest a type II conformation for this turn in the cis isomer, in agreement with that observed for the trans isomer.

In the presence of Fab, the trans isomer displays TRNOEs that are more intense and display broader line widths than their corresponding NOEs (Figure 4B). The increased intensity and line width of the TRNOE is a consequence of the longer local correlation times associated with the bound state ($\tau_{ijB} > \tau_{ijF}$). This results in faster cross-relaxation between proton pairs ($W_{ijB} \gg W_{ijF}$), increased contribution of $P_B W_{ijB}$ to TRNOE$_{ij}$, and increased line width ($\Delta\nu_{obs} > \Delta\nu_F$) (see eqs 3 and 4). In contrast to the trans isomer, the cis isomer displays many TRNOEs that are weaker in intensity than their corresponding NOEs (Figure 5B). Although it is counter-intuitive that a TRNOE can decrease in intensity from its original NOE, line broadening may contribute to this effect by significantly decreasing the height and therefore the measured intensity of the peak. Thus, although TRNOE enhancements are also present for the cis isomer, significant line broadening of the weak cis resonances might bring intensity levels below the detectable threshold.

Apart from subtle differences in intensity and line width, a careful comparison of the TRNOESY versus NOESY spectra for the trans and cis isomers reveals few *new* TRNOEs that develop in the presence of Fab. Those TRNOEs that do develop (boxed cross-peaks) already exist as NOEs at much weaker intensities and therefore do not represent new connectivities. Thus, it appears as if the free solution conformations of the trans and cis isomers are retained in the bound state. Significantly, the connectivities that define the turns in the absence of Fab are observed at the same relative intensities in the presence of Fab, suggesting that the integrity of the turns are preserved in the antibody combining site. This is consistent with the premise that the turns comprise the structural epitope for PAK-13 recognition (*24*). Interestingly, a small but important TRNOE enhancement is observed for $d_{\alpha N}$(140,142) in the cis isomer (Figure 5B). This connectivity is strongly diagnostic of a $\beta$-turn conformation and clearly indicates that the region spanned by Pro[139]-Lys-Gly-Cys[142] in the cis isomer is bound as a $\beta$-turn.

Although the TRNOESY experiment does not indicate significant Fab-induced changes in the backbone conformation of either the trans or the cis isomer, the TRNOE enhancements associated with Asp[134] ($d_{\beta N}$(133,134), $d_{\gamma N}$(133,134)) and Gln[136] $d_{\alpha N}$(136), $d_{\beta N}$(136), $d_{\alpha N}$(135,136), $d_{\beta N}$(135,136), $d_{\gamma N}$(135,136)) in the trans isomer and Glu[135] ($d_{NN}$(134,135), $d_{\alpha N}$(134,135), $d_{\alpha N}$(135)) and Gln[136] ($d_{\beta N}$(136)) in the cis isomer do indicate significant ordering of the backbone around these residues in the bound state. Assuming that $r_{ijB} \approx r_{ijF}$ for all proton pairs, the magnitude of the TRNOE enhancement is largely determined by the difference between the free and bound correlation times, $\Delta\tau_{ij} = \tau_{ijB} - \tau_{ijF}$. Thus, if a select group of residues undergo preferential ordering upon binding, they should be associated with larger $\Delta\tau_{ij}$ values and larger TRNOE enhancements. The significant TRNOE enhancements associated with Asp[134] and Gln[136] in the first $\beta$-turn of the trans isomer (Asp[134]-Glu-Gln-Phe[137]) therefore suggest that this region of the trans isomer undergoes the greatest ordering upon binding to Fab. This might occur if the two turns were equally immobilized upon Fab binding ($\tau_{ijB}$ first turn $\approx \tau_{ijB}$ second turn), but if the first turn started out as the least ordered of the two in the absence of Fab ($\tau_{ijF}$ first turn $< \tau_{ijF}$ second turn). In support of this theory, $^{15}$N relaxation studies of the trans isomer $^{15}$N-labeled recombinant PAK pilin peptide (*31*) found the first turn to be less ordered than the second turn in the free solution state. In addition, $^{15}$N NMR relaxation studies of the trans isomer in complex with Fab PAK-13 demonstrate greater ordering of the first turn versus the second turn upon binding (*27*).

Similar arguments of preferential ordering may be applied to the TRNOE enhancements observed for the cis isomer, although $^{15}$N-edited NMR studies of the free solution structure of the cis isomer found no evidence for a $\beta$-turn spanning residues Asp[134]-Glu-Gln-Phe[137]. Instead, a weakly populated turn spanning Asp[132]-Gln-Asp-Glu[135] was suggested by the pattern of temperature coefficient, coupling constant, and NOE data (*26*). The present set of experiments cannot determine if the Fab recognizes this weakly populated turn. However, $^{15}$N NMR relaxation studies of the cis isomer in complex with Fab PAK-13 (*27*) demonstrate significant ordering of residues 131−135 upon binding and therefore suggest that this may indeed be the case.

Preferential ordering of the first turn in the trans and cis isomers may not be the sole phenomenon contributing to the observed TRNOE enhancements. If the backbone is allowed to undergo even a subtle change in conformation upon binding to Fab, this could lead to the closer approach of select interproton distances in the bound state ($r_{ijB} < r_{ijF}$), faster $W_{ijB}$ as a function of $r^{-6}$, and increased contribution of $P_B W_{ijB}$ to TRNOE$_{ij}$ as before. However, any conformational changes must be subtle, as the persistence of key connectivities in the "bound" spectrum (+Fab) of the trans isomer clearly indicates retention of a $\beta$-turn of type I conformation across Asp[134]-Glu-Gln-Phe[137]. Indeed, the huge TRNOE enhancement associated with $d_{\beta N}$(135,136) may be interpreted as an increase in the population of type I $\beta$-turn conformation. A decrease in the sequential $d_{\beta N}$(135,136) interproton distance implies a decrease in the $\psi$ angle of Glu[135] from positive values ($\psi_{135} > 0$) to negative values ($\psi_{135} < 0$) (*50*), consistent with $\psi = -60$ for the second residue in a type I turn.[8] Thus, if conformational changes around Asp[134] and Gln[136] accompany binding of the trans isomer to Fab, they appear to preserve and even stabilize the first type I $\beta$-turn.

Thus far, a visual comparison of the $^{15}$N-edited HSQC NOESY versus TRNOESY has revealed some obvious TRNOE enhancements for residues in the first turn of the trans and cis isomer. However, direct measurement of NOE versus TRNOE intensities can reveal more subtle TRNOE effects. Figure 6 plots $I_{(+Fab)}/I_{(-Fab)}$ ratios measured for the trans isomer of recombinant $^{15}$N-labeled PAK pilin in the absence and presence of 0.3 mol equiv of Fab PAK-13. Here, $I_{(-Fab)}$ is the intensity of the NOE in the absence of Fab, whereas $I_{(+Fab)}$ is the intensity of the TRNOE in the presence of Fab. Similar measurements were not made for the cis

[8] $(\phi,\psi)_2(\phi,\psi)_3 = (-60,-30)(-90,0)$ for a type I and $(-60,+120)(+90,0)$ for a type II turn (*51*).

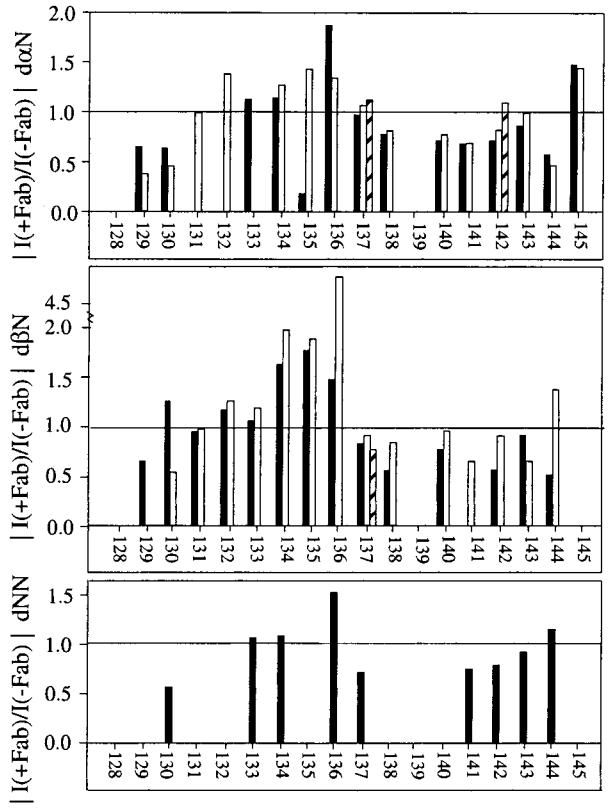


FIGURE 6: Summary of changes in the intensity of $d_{\alpha N}$, $d_{\beta N}$, and $d_{NN}$ connectivities measured for the trans isomer of recombinant $^{15}$N-labeled PAK pilin peptide in the absence and presence of 0.3 mol equiv of Fab PAK-13. Panel A shows $d_{\alpha N}(i,i)$ (black bar), $d_{\alpha N}(i-1,i)$ (white bar), and $d_{\alpha N}(i-2,i)$ (hatched bar) connectivities; panel B shows $d_{\beta N}(i,i)$ (black bar), $d_{\beta N}(i-1,i)$ (white bar), and $d_{\beta N}(i-2,i)$ (hatched bar) connectivities; and panel C shows sequential $d_{NN}(i-1,i)$ (black box) connectivities. Values are given as $I_{(+Fab)}/I_{(-Fab)}$, where $I_{(-Fab)}$ is the intensity of the connectivity in the absence of Fab and $I_{(+Fab)}$ is the intensity of the connectivity in the presence of Fab. The horizontal line in all three panels corresponds to $I_{(+Fab)}/I_{(-Fab)} = 1$. Intensities are measured from the 3D $^{15}$N-edited HSQC NOESY spectra shown in Figure 4 and are not corrected for the effects of dilution and/or precipitation of the peptide-Fab complex. For nondegenerate α or $\beta$ proton connectivities (i.e., $d_{\alpha N}(141,142)$), intensities are averaged before $I_{(+Fab)}/I_{(-Fab)}$ ratios are calculated.

isomer as the poor signal-to-noise associated with the weaker cis resonances precluded quantitative analysis.

Figure 6 reveals significant TRNOE enhancements for the $d_{\alpha N}$, $d_{\beta N}$, and $d_{NN}$ connectivities of residues Asp$^{134}$, Glu$^{135}$, and Gln$^{136}$ in the first type I $\beta$-turn. These enhancements, which range from 20% for $d_{\alpha N}(134)$ to ~500% for $d_{\beta N}(135,136)$, can be clearly visualized in Figure 4 and have already been discussed. Figure 6 also reveals unexpected decreases in TRNOE intensity for the $d_{\alpha N}$, $d_{\beta N}$, and $d_{NN}$ connectivities of residues Cys$^{129}$ and Thr$^{130}$ at the N-terminus and residues Phe$^{137}$, Ile$^{138}$, Lys$^{140}$, Gly$^{141}$, and Cys$^{142}$ spanning the two turns. Interestingly, these residues roughly correspond to those which experienced the greatest chemical shift perturbations in the $^{15}$N-HSQC titrations (Thr$^{130}$, Ser$^{131}$, Phe$^{137}$, Ile$^{138}$, and Cys$^{142}$).

What causes these significant decreases in TRNOE intensity? As previously discussed, a TRNOE can decrease in intensity from its original NOE as a result of linebroadening. One source of this linebroadening is the increased correlation time of the bound state, $\tau_{ijB}$. This leads to faster transverse proton relaxation rates, $1/T_{2B}$, and increased bound proton line width as a function of $\Delta\nu_B = 1/\pi T_{2B}$. Thus, the longer is $\tau_{ijB}$, the larger is the line broadening effect on the measured TRNOE$_{ij}$. This mechanism undoubtedly contributes to the decrease in TRNOE intensity observed for residues spanning the second turn (Pro$^{139}$-Lys-Gly-Cys$^{142}$). Line broadening can also result from chemical exchange between the free and bound states[9] and will be most pronounced for those resonances experiencing the greatest chemical shift perturbations ($\Delta\delta$), for example, Thr$^{130}$ and Ile$^{138}$ in the trans isomer. Finally, line broadening could result from increased conformational exchange in the bound state. Conformational exchange on microsecond to millisecond time scales would contribute an exchange term, $R_{ex}$, to the measured $1/T_{2B}$ rates, which is also manifested as increased bound line width. Recall that $^{15}$N relaxation measurements of the trans isomer at pH 4.5 (*31*) revealed significant conformational exchange around Thr$^{130}$, Gln$^{136}$, Phe$^{137}$, Ile$^{138}$, and Lys$^{140}$ ($R_{ex} = 0.7$, 0.2, 0.9, 1.5, and 1.1 Hz, respectively). As many of these residues correspond to those for which significant decreases in TRNOE intensity were observed (Cys$^{129}$, Thr$^{130}$, Phe$^{137}$, Ile$^{138}$, Lys$^{140}$, Gly$^{141}$, and Cys$^{142}$), conformational exchange in the bound trans isomer must be contributing to this effect. In addition, the similarity of the chemical shift perturbation map to the "line broadening map" suggests that conformational exchange is the underlying mechanism for both.

*Temperature Coefficient Measurements*. To further probe for preferential stabilization of the first turn versus the second turn in the Fab-bound state, temperature coefficients were measured for the trans and cis isomers of recombinant $^{15}$N-labeled PAK pilin peptide in the absence and presence of 0.3 mol equiv of Fab PAK-13 (see Table 2). The temperature dependence of the amide proton chemical shift, or temperature coefficient ($-\Delta\delta/\Delta T$), is often interpreted as a measure of solvent shielding. For unfolded regions of the sequence, temperature coefficients are expected to be $6 \leq -\Delta\delta/\Delta T \leq 10$ ppb/K, indicating that the backbone is freely solvated by water and that no hydrogen bonds are present which would protect the backbone amides from solvent exchange. For folded regions of the sequence, temperature coefficients are expected to decrease to $-\Delta\delta/\Delta T < 5$ ppb/K (*52*), indicating either the presence of a hydrogen bond or a high degree of solvent shielding arising from other secondary or tertiary elements (*53*). Temperature coefficients have also been proposed to reflect temperature-induced shifts in the equilibrium from structured state to random coil state, with retention of a structured population at higher temperatures correlating with lowered $-\Delta\delta/\Delta T$ values (*54*). Thus, both solvent shielding (due to local structure) and shifts in the equilibria between various conformational states (due to local unfolding) must be considered in the interpretation of the temperature coefficient data obtained for the PAK pilin peptide.

The trans isomer in the absence of Fab displays lowered $-\Delta\delta/\Delta T$ values (<5 ppb/K) for the backbone amides of Gln$^{133}$ (4.4 ppb/K), Glu$^{135}$ (4.6 ppb/K), Phe$^{137}$ (4.6 ppb/K), and Cys$^{142}$ (3.6 ppb/K). Solvent shielding can explain the lowered $-\Delta\delta/\Delta T$ values observed for Phe$^{137}$ and Cys$^{142}$, as

[9] Chemical exchange contributes an exchange term, $K_{ex}$, to the observed $1/T_2$ rates, as $1/T_2^{obs} = P_F 1/T_{2F} + P_B 1/T_{2B} + K_{ex}$, where $K_{ex} = P_B P_F (2\pi\Delta\delta)^2 [k_{-1}(1 + P_B/P_F)]^{-1}$ (*41*). This is manifested as increased observed line width.

Table 2: Temperature Coefficients and Coupling Constants for the Trans and Cis Isomers of the Recombinant $^{15}$N-labeled PAK Pilin Peptide in the Absence and Presence of 0.3 Mol Equiv of Fab PAK13

Section A. Trans (pH 4.5, 5.0 °C)

| | $-\Delta\delta/\Delta T \times 1000$[a] | | $^3J_{N\alpha}$ [b] | |
|---|---|---|---|---|
| residue | −Fab (ppb/K) | +Fab (ppb/K) | −Fab (Hz) | +Fab (Hz) |
| Cys[129] | 5.0 | 4.6 | 7.1 | 7.1 |
| Thr[130] | 7.6 | 7.4 | 8.2 | 8.7 |
| Ser[131] | 6.6 | 6.0 | 7.6 | 6.7 |
| Asp[132] | 5.0 | 4.8 | 7.1 | 7.0 |
| Gln[133] | 4.4 | 4.4 | 6.2 | 6.5 |
| Asp[134] | 5.6 | 6.6 | 8.0 | 6.3 |
| Glu[135] | 4.6 | 4.0 | 6.2 | 5.3 |
| Gln[136] | 5.6 | 5.4 | 6.8 | 7.1 |
| Phe[137] | 4.6 | 4.0 | 7.8 | 8.0 |
| Ile[138] | 6.8 | 6.8 | 8.0 | 7.6 |
| Lys[140] | 8.0 | 7.2 | 5.5 | 5.6 |
| Gly[141] | 6.6 | 6.0 | | |
| Cys[142] | 3.6 | 3.4 | 7.5 | 6.6 |
| Ser[143] | 6.4 | 5.6 | 7.3 | 6.9 |
| Lys[144] | 7.6 | 7.0 | 7.3 | 6.8 |
| Hs[145] | 7.0 | 6.4 | 7.3 | 7.1 |

Section B. Cis (pH 4.5, 5.0 °C)

| | $-\Delta\delta/\Delta T \times 1000$ | | $^3J_{N\alpha}$ | |
|---|---|---|---|---|
| residue | −Fab (ppb/K) | +Fab (ppb/K) | −Fab (Hz) | +Fab (Hz) |
| Cys[129] | 4.0 | 3.6 | 7.0 | 7.0 |
| Thr[130] | 9.2 | 9.0 | 10.2 | 13.1 ± 3.1 |
| Ser[131] | 6.2 | 5.4 | 7.3 | |
| Asp[132] | 5.0 | 4.6 | 9.1 | 8.8 |
| Gln[133] | 5.2 | 5.2 | 4.3 | 6.2 ± 1.9 |
| Asp[134] | 6.5 | 5.2 | | |
| Glu[135] | 2.6 | 3.0 | | |
| Gln[136] | 0.6 | 1.0 | | |
| Phe[137] | 9.4 | 9.0 | 9.0 | 7.2 ± 1.9 |
| Ile[138] | 11.4 | 10.8 | | |
| Lys[140] | 7.2 | 6.0 | 2.8 | |
| Gly[141] | 9.6 | 9.0 | | |
| Cys[142] | 2.4 | 2.0 | 6.3 | 5.5 ± 1.2 |
| Ser[143] | 5.0 | 4.8 | 6.9 | 8.0 ± 1.5 |
| Lys[144] | 5.4 | 4.0 | 7.5 | 6.5 ± 2.3 |
| Hs[145] | 5.6 | 5.0 | 7.6 | 8.2 |

[a] Uncertainty in the measured temperature coefficient values is ±0.2 ppb/K. [b] Uncertainty in the measured coupling constants is ±0.3 Hz, unless otherwise noted.

the backbone amides of these residues are involved in (1,4) hydrogen bonds to the carbonyl oxygen of the first residue in the turn (Asp[134] CO- - -Phe[137] NH and Pro[139] CO- - -C[142]NH). However, solvent shielding cannot adequately explain the lowered $-\Delta\delta/\Delta T$ values observed for either Gln[133] or Glu[135], as these residues are not involved in hydrogen bonds, nor are they buried within a solvent-inaccessible pocket (*22*). Thus, temperature-induced shifts in the equilibrium between structured and random coil states must be considered.

The temperature dependence of the $\{^1H\}^{-15}N$ heteronuclear NOE provides one approach for studying these temperature-induced shifts in equilibrium. $\{^1H\}^{-15}N$ NOEs measured for the trans isomer in the absence of Fab at pH 4.5 (*31*) show values significantly larger than the mean for Glu[135], Lys[140], Gly[141], and Cys[142] within the range of 5−15 °C, suggesting retention of backbone structure even as temperatures are raised by 10 °C. This apparent retention of structure at higher temperatures (∼15 °C) should correlate with lowered $-\Delta\delta/\Delta T$ values and appears to do so for both Glu[135] and Cys[142]. However, retention of structure still cannot explain why the $-\Delta\delta/\Delta T$ of Gln[133] in a relatively unordered region of the peptide is low or why the $-\Delta\delta/\Delta T$ of Lys[140] in an ordered region is elevated (8.0 ppb/K). Evidently, the temperature dependence of the amide proton chemical shift is still only partly understood for the PAK pilin system and will remain so until the complex interplay between the temperature dependence of conformational equilibria and the local structure of each conformational state in the system is thoroughly understood.

The cis isomer in the absence of Fab displays lowered $-\Delta\delta/\Delta T$ values for the backbone amides of Cys[129] (4.0 ppb/K), Glu[135] (2.6 ppb/K), Gln[136] (0.6 ppb/K), and Cys[142] (2.4 ppb/K). Again, the small temperature coefficient of the Cys[142] backbone amide may be a consequence of its involvement in the (1,4) hydrogen bond in the second $\beta$-turn. By contrast, the high-temperature coefficient of the backbone amide of Phe[137] (9.4 ppb/K) suggests no involvement of the Phe[137]-NH in a hydrogen bond, consistent with the absence of the first turn spanning Asp[134]-Glu-Gln-Phe[137] (*26*). However, the small temperature coefficients of the Glu[135] backbone amide may be a consequence of its involvement in the (1,4) hydrogen bond in a first $\beta$-turn spanning Asp[132]-Gln-Asp-Glu[135] (*26*). Further interpretation of cis temperature coefficients is not possible as the temperature dependence of the $\{^1H\}^{-15}N$ NOE has not been measured for this isomer, nor has the NMR solution structure been solved.

In the presence of Fab, the bound state will contribute to the observed temperature coefficient, $-\Delta\delta/\Delta T_{obs}$, in a population weighted manner:

$$-\Delta\delta/\Delta T_{obs} = P_B(-\Delta\delta/\Delta T_B) + P_F(-\Delta\delta/\Delta T_F) \quad (5)$$

so that significant differences between $-\Delta\delta/\Delta T_{obs}$ measured in the presence of Fab and $-\Delta\delta/\Delta T_F$ measured in the absence of Fab should reflect the contribution of $-\Delta\delta/\Delta T_B$. The trans isomer displays significant decreases in $-\Delta\delta/\Delta T$ ($|\Delta\delta/\Delta T_F - \Delta\delta/\Delta T_{obs}| > 0.5$ ppb/K) for Ser[131], Glu[135], Phe[137], Lys[140], Gly[141], Ser[143], Lys[144], and Hs[145], where the largest decreases are observed for Lys[140] and Ser[143] (both −0.8 ppb/K). The cis isomer displays significant decreases in $-\Delta\delta/\Delta T$ for a slightly different collection of residues: Ser[131], Asp[134], Ile[138], Lys[140], Gly[141], Lys[144], and Hs[145]. Here, the largest decreases are observed for Ser[131] (−0.8 ppb/K), Asp[134] (−1.3 ppb/K), Lys[140] (−1.2 ppb/K), and Lys[144] (−1.4 ppb/K), considerably larger than those observed for the trans isomer. The decreases in $-\Delta\delta/\Delta T$ observed for the trans and cis isomers may reflect increased solvent sequestering as a result of burial within the antibody combining site. However, as the collection of "solvent protected" residues does not comprise a continuous surface on the NMR solution structure of the trans isomer (*22*), it is more probable that shifts in the temperature-dependent equilibrium to a more structured state contribute to these decreases in $-\Delta\delta/\Delta T$. Thus, binding of Fab may serve to stabilize the trans and cis isomers against local unfolding events, where the larger decreases in $-\Delta\delta/\Delta T$ observed for the cis resonances may indicate a greater degree of stabilization for the cis versus the trans isomer.

The temperature coefficient data in the presence of Fab also suggest that the integrity of the (1,4) hydrogen bonds which stabilize the turns in the trans and cis isomers are preserved in the bound state. This is evidenced by the lowered $-\Delta\delta/\Delta T$ values observed in the presence of Fab

for Phe[137] (4.0 ppb/K) and Cys[142] (3.4 ppb/K) in the trans isomer and Glu[135] (3.0 ppb/K) and Cys[142] (2.0 ppb/K) in the cis isomer. Thus, the turns themselves must also be preserved in the bound state, as implied earlier by the TRNOESY results. Interestingly, a significant decrease in $-\Delta\delta/\Delta T$ is observed in the trans isomer for Phe[137] ($-\Delta\delta/\Delta T_B = 4.0$ ppb/K; $-\Delta\delta/\Delta T_F = 4.6$ ppb/K) but not for Cys[142] ($-\Delta\delta/\Delta T_B = 3.4$ ppb/K; $-\Delta\delta/\Delta T_F = 3.2$ ppb/K) in the presence of Fab. Interpreted within the context of hydrogen bonds, this indicates that the Asp[134]CO- - -Phe[137]NH bond is weaker than the Pro[139]CO- - -Cys[142]NH in the absence of Fab, but that the former is significantly more strengthened than the latter in the presence of Fab. Interpreted within the context of temperature-dependent equilibria, this indicates that less stable local structure is found around Phe[137] versus Cys[142] in the absence of Fab, but that the local structure around Phe[137] is more significantly stabilized in the presence of Fab. Regardless of interpretation, the data suggest that the first turn is preferentially stabilized over the second turn in the presence of Fab. This is in agreement with the $^{15}$N-edited HSQC TRNOESY results presented earlier and is supported by $^{15}$N relaxation studies of the trans isomer in the absence (*31*) and presence (*27*) of Fab.

*Coupling Constant Measurements.* The final set of experiments involved measurement of $^3J_{N\alpha}$ backbone coupling constants for the trans and cis isomers of the recombinant $^{15}$N-labeled PAK pilin peptide in the absence and presence of 0.3 mol equiv of Fab PAK-13 (see Table 2). These measurements should detect local changes in the backbone conformations of the trans and cis isomers caused by Fab binding. The trans isomer in the absence of Fab displays $^3J_{N\alpha}$ values of $\geq$8 Hz, consistent with a $\phi$ angle in extended or $\beta$-strand dihedral space, for Thr[130] (8.2 Hz), Asp[134] (8.0 Hz), and Ile[138] (8.0 Hz). $^3J_{N\alpha}$ values of $\leq$6 Hz, consistent with the $\phi_2$ angle of a type II $\beta$-turn, are observed for Lys[140] (5.5 Hz). The cis isomer in the absence of Fab displays $^3J_{N\alpha}$ values of $\geq$8 Hz, consistent with a $\phi$ angle in extended or $\beta$-strand dihedral space for Thr[130] (10.2 Hz), Asp[132] (9.1 Hz), and Phe[137] (9.0 Hz). $^3J_{N\alpha}$ values of $\leq$ 6Hz, consistent with a $\phi_2$ angle of a type I or II $\beta$-turn are observed for Gln[133] (4.3 Hz) and Lys[140] (2.8 Hz).

Similar to eq 5, the bound state will contribute to the observed coupling constant, $^3J_{N\alpha\,obs}$, in a population weighted manner:

$$^3J_{N\alpha\,obs} = P_B(^3J_{N\alpha B}) + P_F(^3J_{N\alpha F}) \qquad (6)$$

so that $^3J_{N\alpha\,obs}$ should reflect the structure of the bound state. Significant decreases in $^3J_{N\alpha}$ ($^3J_{N\alpha F} - {}^3J_{N\alpha\,obs} > 0.6$ Hz) were measured for several residues in the trans isomer including Ser[131], Asp[134], Glu[135], and Cys[142]. These decreases in $^3J_{N\alpha}$ reflect decreases in the $\phi$ dihedral angles for these residues (*50*). Thus, the decreases in $\phi$ measured for Asp[134] and Glu[135] in the first type I $\beta$-turn of the trans isomer may reflect a decrease in the population of extended structure for the first turn. This is consistent with preferential stabilization of the first turn in the presence of Fab. Notice also that the $^3J_{N\alpha}$ coupling constant for Glu[135] in position 2 of the type I $\beta$-turn decreases from 6.2 to 5.3 Hz upon binding to Fab, consistent with a higher population of turn conformation in solution. By contrast, the $^3J_{N\alpha}$ coupling constant for Lys[140] in position 2 of the type II $\beta$-turn does not significantly change in the presence of Fab (5.5 Hz in the absence vs 5.6 Hz in the presence of Fab). This suggests that the population of this turn in solution, already well-populated in the absence of antibody, does not significantly change in the presence of antibody.

Using a method developed by Yao et al. (*55*), turn populations may be estimated from the $^3J_{N\alpha}$ coupling constants measured for the residues in position 2 of the two turns, i.e., Glu[135] and Lys[140]. A two-site model is used in which residues Glu[135] and Lys[140] can find themselves in either a turn conformation or in an extended conformation. Assuming 100% turn conformation, the coupling constants for Glu[135] and Lys[140] should be $^3J_{N\alpha} = 4$ Hz, corresponding to $\phi_2 = -60$ (*56*). Assuming 100% extended conformation, coupling constants of $^3J_{N\alpha} = 9$ Hz are expected, corresponding to $\phi_2 < -100$ (*56*). From these two extreme values of $^3J_{N\alpha}$, the measured $^3J_{N\alpha}$ values were used to roughly estimate the percentage of turn for residues Glu[135] and Lys[140] in the absence and presence of 0.3 mol equiv of Fab PAK-13. Values are obtained of 56% and 74% for the first turn in the absence and presence of Fab, respectively, and of 70% and 68% for the second turn in the absence and presence of Fab, respectively.

## SUMMARY OF RESULTS

$^{15}$N-edited NMR studies of a $^{15}$N-labeled recombinant PAK pilin peptide in complex with the Fab fragment of monoclonal antibody PAK-13 were performed. These studies used a combination of chemical shift perturbation mapping, TRNOESY experiments, and measurement of coupling constants and temperature coefficients to probe for antibody-induced changes in the backbone conformations of the trans and cis isomers of the PAK pilin peptide. Several major conclusion can be drawn from these studies:

(i) Both the trans and the cis isomer of the PAK pilin peptide bind to Fab PAK-13 with apparently similar affinities. This may be due to the presence of the type II $\beta$-turn spanning Pro[139]-Lys-Gly-Cys[142] in both isomers. However, additional features must also contribute to PAK-13 binding (such as the first turn in each isomer), as a different pattern of backbone perturbations is observed for each isomer, suggesting that different "surfaces" interact with the Fab in each case.

(ii) Binding of Fab PAK-13 does not appear to significantly alter the backbone conformations of either the trans or the cis isomer. This is especially true for the turn regions: a comparison of NOESY (−Fab) versus TRNOESY (+Fab) connectivities shows that the placement and conformation of the turns in the trans and cis isomers (a type I $\beta$-turn spanning Asp[134]-Glu-Gln-Phe[137] and a type II $\beta$-turn spanning Pro[139]-Lys-Gly-Cys[142] in the trans isomer; a type II $\beta$-turn spanning Pro[139]-Lys-Gly-Cys[142] in the cis isomer) are unaltered by Fab binding. Thus, the free solution conformation of the turns are preserved in the antibody combining site.

(iii) Binding of Fab PAK-13 leads to preferential stabilization of the first turn (Asp[134]-Glu-Gln-Phe[137]) over the second turn (Pro[139]-Lys-Gly-Cys[142]) in the trans isomer. This may result from a lower free state population for the first turn. If the two turns were to equally constitute the structural epitope for PAK-13 binding (bound state populations are the same

for each turn), the first turn will experience the greatest increase in population and will therefore appear to be the more stabilized of the two. Preferential stabilization of the first turn in the cis isomer may also occur, but is not clearly indicated.

(*4*) Binding of Fab PAK-13 to the trans isomer leads to the perturbation (shifting, line broadening) of resonances within regions of the backbone that undergo microsecond to millisecond "exchange-related" motions in the free solution state. These regions are spanned by the following residues: $Thr^{130}$ near the disulfide bridge and $Glu^{135}$, $Gln^{136}$, $Phe^{137}$, $Ile^{138}$, and $Lys^{140}$ within the turns.

## DISCUSSION AND CONCLUSIONS

*Role of the β-Turns in PAK Pilin Peptide Immunogenicity.* Our NMR studies of the $^{15}$N-labeled recombinant PAK pilin peptide in complex with the Fab PAK-13 suggest that the β-turns comprise the structural motif for antibody recognition and maintain their free solution conformations when bound in the antibody combining site. The discovery of the immunogenic importance of the β-turn in the pilin system is supported by other research groups in other systems. NMR solution studies of antigenic peptides in their free versus antibody bound states have shown that stable β-turns are present in these peptides (*22, 23, 26, 57*−*67*) and that the turns provide the primary contact interface for antibody recognition (*24, 68*−*73*). X-ray crystal studies of antibody peptide-complexes consistently find one, two, or even three peptide β-turns at the antibody interface (*74*−*90*). In this regard, 13 of the 16 unique X-ray crystal structures of antibody−peptide complexes available in the PDB show peptide turns deeply embedded in the antibody combining site; the other three structures show the peptide in an extended conformation.[10] Thus, the β-turn appears to be *the* most important structural motif for antibody−peptide recognition and may be a key feature in the design of a synthetic pilin peptide vaccine capable of elliciting a strong humoral immune response against the intact bacterial pilus.

Interestingly, both the trans and cis isomers bind with apparently equal affinity to Fab PAK-13, although their only shared structural feature is the type II β-turn spanning $Pro^{139}$-Lys-Gly-$Cys^{142}$. This conserved turn is well-populated in the free solution state of both isomers and does not undergo significant stabilization upon Fab binding. By contrast, the first turns in the trans ($Asp^{134}$-Glu-Gln-$Phe^{137}$) and cis ($Asp^{133}$-Gln-Asp-$Glu^{135}$) isomers are less well-populated in the free solution state but undergo significant stabilization upon Fab binding (clearly observed for the trans isomer). Thus, binding of the first turn appears to involve an "induced-fit" mechanism for the first turn. This mechanism might allow the PAK-13 combining site to accommodate either a trans or cis topology, although the relative distance and orientation of the first to the second turn are different in each isomer.

*Role of Slow Backbone Motions in PAK Pilin Peptide Immunogenicity.* Motions that appear to have the greatest significance in creating an induced fit are those within the microsecond to millisecond time scale or slow motions involving conformational exchange (*92*). Many groups have found that active sites or binding pockets of proteins experience conformational exchange processes, which are either stabilized (*93*−*96*) or increased (*97*−*100*) by ligand binding, thereby increasing or decreasing the loss of entropy upon binding. Conformational exchange may therefore provide a mechanism for modulating available intrinsic binding energy, preserving moderate affinities for optimal biological function.

The NMR studies of the recombinant $^{15}$N-labeled PAK pilin peptide in complex Fab PAK-13 presented here demonstrate significant chemical shift perturbation and line broadening for backbone resonances of residues within the turns or near the disulfide bridge. $^{15}$N NMR relaxation experiments of the trans isomer of the recombinant $^{15}$N-labeled PAK pilin peptide in the absence of PAK-13 Fab (*31*) showed slow motions on the microsecond to millisecond time scale for $Thr^{130}$ near the disulfide bridge and for $Glu^{135}$, $Gln^{136}$, $Phe^{137}$, $Ile^{138}$, and $Lys^{140}$ within the turns. $^{15}$N NMR relaxation experiments of the trans isomer in the presence of PAK-13 Fab show that these microsecond to millisecond time scale motions are partially stabilized in the bound state (*27*). Thus, the most plastic regions of the sequence appear to be the regions most perturbed and/or stabilized upon antibody binding. These observations are consistent with an induced-fit model for antibody recognition of PAK pilin peptide.

Significantly, the residue in the trans isomer for which the greatest backbone perturbations were observed was $Ile^{138}$. This residue is also the site of the greatest conformational exchange measured from previous $^{15}$N NMR relaxation experiments of the trans isomer in the absence (*31*) and presence (*27*) of Fab. $Ile^{138}$ is a "hinge" residue for cis/trans isomerization ($Ile^{138}$-$Pro^{139}$) and is situated immediately before the second type II β-turn ($Pro^{139}$-Lys-Gly-$Cys^{142}$) in both the trans and cis isomers. Hinge motions around $Ile^{138}$, detected as slow time scale conformational exchange in an NMR experiment, could conceivably bring the two turns in the trans and cis isomers into the same relative alignment for binding. This would allow PAK-13 to accommodate the different topologies of the two isomers with apparently similar binding affinities. The following sequence of binding events presents a mechanism whereby this might occur. First, the well-ordered second turn binds within the antibody combining site. Second, rotation around one or both of the dihedral angles ($\phi$ or $\psi$) of $Ile^{138}$ brings the first turn into the proper alignment for binding. Third, the less-ordered first turn binds within the antibody combining site, where it is stabilized through energetically favorable antibody−peptide interactions. This three-step mechanism, while speculative, illustrates how slow time scale conformational exchange might modulate induced fit binding of the first turn in the PAK pilin system and accounts for the ability of the PAK-13 antibody to bind both the trans and the cis isomers with similar affinities.

[10] Interestingly, a survey of the Fab-peptide X-ray crystal structures available in the PDB shows a relationship between the length of the H3 loop and the conformation of the bound peptide (*91*). For H3 loops equal to or longer than seven residues, the bound peptides are found to be in a β-turn conformation, in which the turn is buffered against either the N- or the C-terminal edge of the H3 loop. For H3 loops equal to or less than six residues (less common), the bound peptides are found to be in an extended conformation, lying across the top of the H3 loop. The NMR or X-ray structure of Fab PAK-13 has yet to be determined, thus the length of the H3 loop in the PAK-13 combining site is unknown at the present time.

From a broader immunological perspective, conformational exchange may also play a role in induced fit binding of different pilin immunogens to PAK-13, providing a mechanism for antibody cross-reactivity. For example, PAK-13 was raised against the intact PAK pilus yet recognizes and binds to the intact pilus from other strains of *P. aeruginosa*, including PAO, KB7, and P1 (*28*). PAK-13 also binds with similar affinities (micromolar) to the PAK, PAO, KB7, and P1 pilin peptides derived from the C-terminal receptor binding regions of the pilin proteins of these parent strains (*24*). This cross-reactivity has been proposed to arise from the existence of conserved set of $\beta$-turns (*22*, *23*), which comprise the primary structural epitope for the interaction of each peptide with PAK-13 (*28*). Interestingly, the relative orientations of the first to the second turn differ significantly from one peptide structure to the next (*22, 23*).[11] Thus, PAK-13 appears to be able to accommodate the different topologies of each peptide with no apparent loss in affinity. While some of this cross-reactivity may be attributed to the plasticity of the PAK-13 combining site itself, some may also be attributed to conformational exchange within the peptide sequences. If a site for slow time scale hinge motions (analagous to the Ile$^{138}$ "hinge" site in the cis and trans isomers of PAK) is allowed to exist between the first and second turns in each of the PAO, KB7, and P1 pilin peptides, dihedral angle rotations around this putative site could bring the first and second turns of each peptide into the same relative alignment for binding. Thus, slow time scale hinge motions may be a general property of all pilin sequences and not just a unique phenomenon limited to the PAK pilin system. This is intriguing from the perspective of vaccine design, as it may provide the basis for the generation of an antibody therapeutic effective against the multiple strains of *P. aeruginosa*. Clearly, $^{15}$N NMR relaxation experiments of recombinant $^{15}$N-labeled versions of the PAO, KB7, and P1 pilin peptides are required to explore this possibility, as these experiments would detect and measure any significant slow time scale conformational exchange processes in each of these peptides.

*Significance to Peptide Vaccine Design.* Since the $\beta$-turns in the pilin system have been implicated in antibody recognition (*24*), features designed to stabilize the turns should result in increased antibody affinity and enhanced immunogenicity. In fact, conformationally constraining peptide antigens to stabilize $\beta$-turns has been shown in practice to increase antibody affinity (*61, 101, 102*). However, design strategies that constrain a peptide immunogen into the desired conformation strive toward the lock-and-key model of binding in which antibody affinity and specificity are theoretically maximized. Were our goal to design a strain-specific PAK peptide vaccine effective against *P. aeruginosa* strain K infections only, the next logical step might be the design of constrained PAK peptide analogues or even peptidomimetics. However, our goal is cross-protection against a broad spectrum of *P. aeruginosa* strains, so design strategies must instead strive toward the induced fit model, in which the dynamics of the free and bound states modulate binding energy and allow for cross-reactivity in recognition and binding. To this end, a detailed picture of the dynamics involved in antibody recognition of pilin immunogens is a necessary component of vaccine design, providing critically important information to the generation of an immune response effective against the multiple strains of *P. aeruginosa*.

[11] The NMR free solution structures of the PAK, PAO, KB7, and P1 pilin peptides correspond to the trans isomers of these peptides (*22, 23*). It should also be noted that while the PAK pilin peptide undergoes cis/trans isomerization around the central Ile$^{138}$-Pro$^{139}$ peptide bond, the PAO, KB7, and P1 peptides, which all contain one or more prolines in their sequence, adopt an exclusively trans conformation around each X-Pro bond (*22, 23*).

## ACKNOWLEDGMENT

The authors thank Paul Semchuck for mass spectrometry; Stéphane Gagné for NMR assistance with the heteronuclear pulse sequences; Robert Boyko, Tim Jellard, and Leigh Willard for computer programming assistance; Marie Kaplan for competitive ELISA experiments and antibody concentration determinations; and Niels Andersen for helpful discussions of temperature coefficients in polypeptides. The BL21(DE3) cells were a generous gift provided by Dr. Joyce Pearlstone.

## REFERENCES

1. Rivera, M., and Nicotra, M. B. (1982) *Am. Rev. Respir. Dis. 126*, 833−836.
2. Pier, G. B. (1985) *J. Infect. Dis. 151*, 575−580.
3. Todd, T. R. J., Franklin, A., Mankinen-Irvin, P., Gurman, G., and Irvin, R. T. (1989) *Am. Rev. Respir. Dis. 140*, 1585−1589.
4. Sajjan, U., Reisman, J., Doig, P., Irvin, R. T., Forstner, G., and Forstner, J. (1991) *J. Clin. Invest. 89*, 657−665.
5. Irvin, R. T. (1993) in *Pseudomonas Aeruginosa as an Opportunistic Pathogen* (Campa, M., Ed.) pp 19−42, Plenum Press, New York.
6. Paranchych, W., Sastry, P. A., Volpel, K., Loh, B. A., and Speert, D. P. (1986) *Clin. Invest. Med. 9*, 113−118.
7. Ramphal, R., Sadoff, J. C., Pyle, M., and Silipigni, J. D. (1984) *Infect. Immun. 44*, 38−40.
8. Doig, P., Smith, N. R., Todd, T., and Irvin, R. T. (1987) *Infect. Immun. 55*, 1517−1522.
9. Doig, P., Todd, T., Sastry, P. A., Lee, K. K., Hodges, R. S., Paranchych, W., and Irvin, R. T. (1988) *Infect. Immun. 56*, 1641−1646.
10. Doig, P., Sastry, P. A., Hodges, R. S., Lee, K. K., Paranchych, W., and Irvin, R. T. (1990) *Infect. Immun. 58*, 124−130.
11. Irvin, R. T., Doig, P., Lee, K. K., Sastry, P. A., Paranchych, W., Todd, T., and Hodges, R. S. (1989) *Infect. Immun. 57*, 3720−3726.
12. Lee, K. K., Doig, P., Irvin, R. T., Paranchych, W., and Hodges, R. S. (1989) *Mol. Microbiol. 3*, 1493−1499.
13. Lee, K. K., Sheth, H. B., Wong, W. Y., Sherburne, R., Paranchych, W., Hodges, R. S., Lingwood, C. A., Krivan, H., and Irvin, R. T. (1994) *Mol. Microbiol. 11*, 705−713.
14. Krivan, H. C., Ginsburg, V., and Roberts, D. D. (1988) *Arch. Biochem. Biophys. 260*, 493−496.
15. Krivan, H. C., Roberts, D. D., and Ginsburg, V. (1988) *Proc. Natl. Acad. Sci. U.S.A. 85*, 6157−6161.
16. Baker, N., Hansson, G. C., Leffler, H., Riise, G., and Svanborg-Eden, C. (1990) *Infect. Immun. 58*, 2361−2366.
17. Ramphal, R., Carnoy, C., Fievre, S., Michalski, J.-C., Houdret, N., Lamblin, G., Strecker, G., and Roussel, P. (1991) *Infect. Immun. 59*, 700−704.
18. Sheth, H. B., Lee, K. K., Wong, W. Y., Srivastava, G., Hindsgaul, O., Hodges, R. S., Paranchych, W., and Irvin, R. T. (1994) *Mol. Microbiol. 11*, 715−723.
19. Lee, K. K., Paranchych, W., and Hodges, R. S. (1990) *Infect. Immun. 58*, 2727−2732.
20. Lee, K. K., Yu, L., Macdonald, D. L., Paranchych, W., Hodges, R. S., and Irvin, R. T. (1996) *Can. J. Microbiol. 42*, 479−486.

21. Yu, L., Lee, K. K., Paranchych, W., Hodges, R. S., and Irvin, R. T. (1996) *Mol. Microbiol. 19*, 1107−1116.
22. Campbell, A. P., McInnes, C., Hodges, R. S., and Sykes, B. D. (1995) *Biochemistry 34*, 16255−16268.
23. Campbell, A. P., Sheth, H. B., Hodges, R. S., and Sykes, B. D. (1996) *Int. J. Pept. Protein Res. 38*, 539−552.
24. Campbell, A. P., Wong, W. Y., Houston, M. E., Jr., Schweizer, F., Cachia, P. J., Irvin, R. T., Hindsgaul O., Hodges, R. S., and Sykes, B. D. (1997) *J. Mol. Biol. 267*, 382−402.
25. Tripet, B., Yu, L., Bautista, D. L., Wong, W. Y., Irvin, R. T., and Hodges, R. S. (1996) *Protein Eng. 9*, 1029−1042.
26. Campbell, A. P., Bautista, D. L., Tripet, B., Irvin, R. T., Hodges, R. S., and Sykes, B. D. (1997) *Biochemistry 36*, 12791−12801.
27. Campbell, A. P., Spyracopoulos, L., Wong, W. Y., Irvin, R. T., and Sykes, B. D. (2000) manuscript in preparation.
28. Sheth, H. B., Glasier, L. M. G., Ellert, N. W., Cachia, P., Kohn, W., Lee, K. K., Paranchych, W., Hodges, R. S., and Irvin, R. T. (1995) *Biomed. Pept., Proteins, Nucleic Acids 1*, 141−148.
29. Wong, W. Y., Irvin, R. T., Paranchych, W., and Hodges, R. S. (1992) *Protein Sci. 1*, 1308−1318.
30. Nieto, A., Gaya, A., Jansa, M., Moreno, C., and Vives, J. (1984) *Mol. Immunol. 21*, 537−543.
31. Campbell, A. P., Spyracopoulos, L., Irvin, R. T., and Sykes, B. D. (2000) *J. Biomol. NMR 17*, 239−255.
32. Kay, L. E., Keifer, P., and Saarinen, T. (1992) *J. Am. Chem. Soc. 114*, 10663−10665.
33. Muhandiram, D. R., and Kay, L. E. (1994) *J. Magn. Reson. B103*, 203−216.
34. Zhang, O., Kay, L. E., Olivier, J. P., and Forman-Kay, J. D. (1994) *J. Biomol. NMR 4*, 845−858.
35. Zuiderweg, E. R., and Fesik, S. W. (1989) *Biochemistry 28*, 2387−2391.
36. Vuister, G. W., and Bax, A. (1993) *J. Am. Chem. Soc. 115*, 7772−7777.
37. Garrett, D. S., Powers, R., Gronenborn, A. M., and Clore, G. M. (1991) *J. Magn. Reson. 95*, 214−220.
38. Marion, D., Kay, L. E., Sparks, S. W., Torchia, D. A., and Bax, A. (1989) *J. Am. Chem. Soc. 111*, 1515−1517.
39. Zhu, G., and Bax, A. (1992) *J. Magn. Reson. 100*, 202−207.
40. Campbell, A. P., and Sykes, B. D. (1993) *Annu. Rev. Biophys. Biomol. Struct. 22*, 99−122.
41. Lian, L. Y., Barsukov, I. L., Sutcliffe, M. J., Sze, K. H., and Roberts, G. C. K. (1994) *Methods Enzymol. 239*, 657−700.
42. Schmiedeskamp, M., Rajagopal, P., and Klevit, R. E. (1997) *Protein Sci. 6*, 1835−1848.
43. Foster, M. P., Wuttke, D. S., Clemens, K. R., Jahnke, W., Radhakrishnan, I., Tennant, L., Reymond, M., Chung, J., and Wright, P. E. (1998) *J. Biomol. NMR 12*, 51−71.
44. Radhakrishnan, I., Pèrez-Alvarado, G. C., Parker, D., Dyson, H. J., Montminy, M. R., and Wright. P. E. (1999) *J. Mol. Biol. 287*, 859−865.
45. La Planche, L. A., and Rogers, M. T. (1964) *J. Am. Chem. Soc. 86*, 337−341.
46. Maia, H. L., Orrell, K. G., and Rydon, H. N. (1971) *Chem. Commun.*, 1209−1210.
47. Love, A. L., Alger, T. D., and Olson, R. K. (1972) *J. Phys. Chem. 76*, 853−855.
48. Wüthrich, K., Billeter, M., and Braun, W. (1984) *J. Mol. Biol. 180*, 715−740.
49. Wagner, G., Neuhaus, D., Wôrgôtter, E., Vasák, M., Kägi, J. H. R., and Wüthrich, K. (1986) *J. Mol. Biol. 187*, 131−135.
50. Wüthrich, K. (1986) in *NMR of Proteins and Nucleic Acids*, John Wiley and Sons, New York.
51. Richardson, J. S. (1981) *Adv. Protein Chem. 34*, 167−339.
52. Rose, G. D., Gierasch, L. M., and Smith, J. A. (1985) *Adv. Protein Chem. 37*, 1−109.
53. Watts, C. R., Tessmer, M. R., and Kallick, D. A. (1995) *Lett. Pept. Sci. 2*, 59−70.
54. Andersen, N. H., Neidigh, J. W., Harris, S. M., Lee, G. M., Liu, Z., and Tong, H. (1997) *J. Am. Chem. Soc. 119*, 8547−8561.
55. Yao, J., Feher, V. A., Espejo, B. F., Reymond, M. T., Wright, P. E., and Dyson, H. J. (1994) *J. Mol. Biol. 243*, 736−753.
56. Pardi, A., Billeter, M., and Wüthrich, K. (1984) *J. Mol. Biol. 180*, 741−751.
57. Dyson, H. J., Cross, K. J., Houghten, R. A., Wilson, I. A., Wright, P. E., and Lerner, R. A. (1985) *Nature 318*, 480−483.
58. Dyson, H. J., Rance, M., Houghten, R. A., Lerner, R. A., and Wright, P. E. (1988) *J. Mol. Biol. 201*, 161−200.
59. Dyson, H. J., Rance, M., Houghten, R. A., Wright, P. E., and Lerner, R. A. (1988) *J. Mol. Biol. 201*, 201−217.
60. Chandrasekhar, K., Profy, A. T., and Dyson, H. J. (1991) *Biochemistry 30*, 9187−9194.
61. Blumenstein, M., Matsueda, G. R., Timmons, S., and Hawiger, J. (1992) *Biochemistry 31*, 10692−10698.
62. Zvi, A., Hiller, R., and Anglister, J. (1992) *Biochemistry 31*, 6972−6979.
63. McInnes, C., Sönnichsen, F. D., Kay, C. M., Hodges, R. S., and Sykes, B. D. (1993) *Biochemistry 32*, 13432−13440.
64. De Lorimier, R., Moody, M. A., Haynes, B. F, and Spicer, L. D. (1994) *Biochemistry 33*, 2055−2062.
65. Campbell, A. P., Sykes, B. D., Norrby, E., Assa-Munt, N., and Dyson, H. J. (1996) *Folding Des. 1*, 157−165.
66. Vu, H. M., de Lorimier, R., Moody, A., Haynes, B. F., and Spicer, L. D. (1996) *Biochemistry 35*, 5158−5165.
67. Molins, M. A., Contreras, M. A., Fits, I., and Pona, M. (1998)- *J. Pept. Sci. 4*, 101−110.
68. Scherf, T., Hiller, R., Naider, F., Levitt, M., and Anglister, J. (1992) *Biochemistry 31*, 6884−6897.
69. Zvi, A., Kustanovich, I., Feigelson, D., Levy, R., Eisenstein, M., Matsushita, S., Richalet-Sécordel, P., Regenmortel, M. H. V., and Anglister, J. (1995) *Eur. J. Biochem. 229*, 178−187.
70. Gizachew, D., Moffett, D. B., Busse, S. C., Westler, W. M., Dratz, E. A., and Teintze, M. (1998) *Biochemistry 37*, 10616−10625.
71. Weliky, D. P., Bennett, A. E., Zvi, A., Anglister, J., Steinbach, P. J., and Tycko, R. (1999) *Nat. Struct. Biol. 6*, 141−145.
72. Tugarinov, V., Zvi, A., Levy, R., and Anglister, J. (1999) *Nat. Struct. Biol. 6*, 331−335.
73. Zvi, A., Tugarinov, V., Faiman, G. A., Horovitz, A., and Anglister, J. (2000) *Eur. J. Biochem 267*, 767−779.
74. Stanfield, R. L., Fieser, T. M., Lerner, R. A., and Wilson, I. A. (1990) *Science 248*, 712−719.
75. Rini, J. M., Schulze-Gahmen, U., and Wilson, I. A. (1992) *Science 255*, 959−965.
76. Garcia, K. C., Ronco, P. M., Verroust, P. J., Brunger, A. T., and Amzel, L. M. (1992) *Science 257*, 502−507.
77. Stanfield, R. L., Takimoto-Kamimura, M., Rini, J. M., Profy, A. T., and Wilson, I. A. (1993) *Structure 1*, 83−93.
78. Shoham, M. (1993) *J. Mol. Biol. 232*, 1169−1175.
79. Schulze-Gahmen, U., Rini, J. M., and Wilson, I. A. (1993) *J. Mol. Biol. 234*, 1098−1118.
80. Ghiara, J. B., Stura, E. A., Stanfield, R. L., Profy, A. T., and Wilson, I. A. (1994) *Science 264*, 82−85.
81. Churchill, M. E. A., Stura, E. A., Pinilla, C., Appel, J. R., Houghten, R. A., Kono, D. H., Balderas, R. S., Fieser, G. G., Schulze-Gahmen, U., and Wilson, I. A. (1994) *J. Mol. Biol. 241*, 534−556.
82. Tormo, J., Blass, D., Parry, N. R., Rowlands, D., Stuart, D., and Fita, I. (1994) *EMBO J. 13*, 2247−2256.
83. Stigler, R.-D., Rüker, F., Katinger, D., Elliott, G., Höhne, W., Henklein, P., Ho, J. X., Keeling, K., Carter, D. C., Nugel, E., Kramer, A., Porstmann, T., and Schneider-Mergener, J. (1995) *Protein Eng. 8*, 471−479.
84. Wien, M. W., Filman, D. J., Stura, E. A., Guillot, S., Delpeyroux, F., Crainic, R., and Hogle, J. M. (1995) *Struct. Biol. 2*, 232−243.
85. Verdaguer, N., Mateu, M. G., Andreu, D., Giralt, E., Domingo, E, and Fita, I. (1995) *EMBO J. 14*, 1690−1696.
86. Van den Elsen, J. M. H., Herron, J. N., Hoogerhout, P., Poolman, J. T., Boel, E., Logtenberg, T., Wilting, J., Crommelin, D. J. A., Kroon, J., and Gros, P. (1997) *Proteins 29*, 113−125.
87. Lescar, J., Stouracova, R., Riottot, M.-M., Chitarra, V., Brynda, J., Fabry, M., Horejsi, M., Sedlacek, J., and Bentley, G. A. (1997) *J. Mol. Biol. 267*, 1207−1222.

88. Derrick. J. P., Maiden, M. C. J., and Feavers, I. M. (1999) *J. Mol. Biol. 293*, 81−91.
89. Stanfield, R. L., Cabezas, E., Satterthwait, A. C., Stura, E. A., Profy, A. T., and Wilson, I. A. (1999) *Structure 7*, 131−142.
90. Ochoa, W. F., Kalko, S. G., Mateu, M. G., Gomes, P., Andreu, D., Domingo, E., Fita, I., and Verdaguer, N. (2000) *J. Gen. Virol. 81*, 1495−1505.
91. Bates, P. A., Dokurno, P., Freemont, P. A., and Sternberg, M. J. E. (1998) *J. Mol. Biol. 284*, 549−555.
92. Carr, P. A., Erickson, H. P., and Palmer, A. G. (1997) *Structure 5*, 949−959.
93. Nicholson, L. K., Kay, L. E., Baldisseri, D. M., Arango, J., Young, P. E., Bax, A., and Torchia, D. A. (1992) *Biochemistry 31*, 5253−5263.
94. Akke, M., Skelton, J. H., Kordel, J., Palmer, A. G., and Chazin, W. J. (1993) *Biochemistry 32*, 9832−9844.
95. Davis, J. H., Agard, D. A., Handel, T. M., and Basus, V. J. (1997) *J. Biomol. NMR 10*, 21−27.
96. Davis, J. H., and Agard, D. A. (1998) *Biochemistry 37*, 7696−7707.
97. Farrow, N. A., Muhandiram, R., Singer, A. U., Pascal, S. M., Kay, C. M., Gish, G., Shoelson, S. E., Pawson, R., Forman-Kay, J. D., and Kay, L. E. (1994) *Biochemistry 33*, 5984−6003.
98. Epstein, D. M., Benkovic, S. J., and Wright, P. E. (1995) *Biochemistry 34*, 11037−11048.
99. Stivers, J. T., Abeygunawardana, C., and Mildvan, A. S. (1996) *Biochemistry 35*, 16036−16047.
100. Hyre, D. E., and Klevit, R. E. (1998) *J. Mol. Biol. 279*, 929−943.
101. Hinds, H. G., Welsh, J. H., Brennand, D. M., Fisher, J., Glennie, M. J., Richards, H. G. J., Turner, D. L., and Robinson, J. A. (1991) *J. Med. Chem. 34*, 1777−1789.
102. Ghiara, J. B., Ferguson, D. C., Satterthwait, A. C., Dyson, H. J., and Wilson, I. A. (1997) *J. Mol. Biol. 266*, 31−39.

BI0016568